ADVANCES IN ATOMIC, MOLECULAR, AND OPTICAL PHYSICS, VOL. 42

COHERENT CONTROL OF ATOMIC, MOLECULAR, AND ELECTRONIC PROCESSES

MOSHE SHAPIRO
Department of Chemical Physics, The Weizmann Institute, Rehovot, Israel

PAUL BRUMER
Chemical Physics Theory Group, Department of Chemistry, University of Toronto, Toronto, Canada

I. Introduction

One of the central questions in the physical sciences is the extent to which the present determines the future. Quantum mechanics, although a probabilistic theory, gives a deterministic answer to this question: given the wavefunction of an isolated system in the present, the system wavefunction in the future is

ISBN 0-12-003842-0/ISSN 1049-250X/00 $30.00

completely determined. This is a consequence of the fact that the Schrödinger equation is a first-order differential equation in the time variable.

Thus, if we wish to *predict* future probabilities, all we need to do is numerically solve the time-dependent Schrödinger equation, propagating from the present to the future. In spite of the obvious practical difficulties in applying such a program to many-body problems, there is in principle no reason why this cannot be done. Indeed, current methods enable the numerical solution of the time-dependent Schrödinger equation of many (Kosloff, 1988, 1994; Hammerich *et al.*, 1994; Zhang and Miller, 1989; Manolopoulos *et al.* 1991) few- (three- and four-) particle systems. Although a buildup of integration errors with propagation time does occur (Leforestier *et al.*, 1991), the errors are not expected to grow at a faster-than-polynomial rate. This fact is in sharp contradistinction, for example, to the situation in classical mechanics in the chaotic region. In that case, the exponential growth of integration error prevents the numerical determination of the state of the system to acceptable accuracy after the elapse of a sufficiently long time unless the initial phase-space coordinates are known to infinite accuracy.

Given then that the integration of the Schrödinger equation is possible, and that given the present we are able to predict the future probabilities, a more ambitious question can be asked: If we know the initial wavefunction, what dynamics (e.g., what Hamiltonian) guarantees a desirable outcome ("objective") in the future? This question constitutes the essence of the field now called *quantum control.*

In practice, one can modify the Hamiltonian by introducing external fields (e.g., laser light) to alter the dynamics. It is then possible to answer the above question in a "trial-and-error" fashion; we guess a Hamiltonian, propagate the initial wavefunction into the future, compare the result with the desirable objective, and correct the guess for the Hamiltonian until satisfactory agreement with the objective is reached. Indeed, a systematic way of executing this procedure is the subfield called *optimal control* (Gordon and Rice, 1997; Tannor and Rice, 1985; Tannor *et al.*, 1986; Tannor and Rice, 1988; Kosloff *et al.*, 1989; Shi *et al.*, 1988; Shi and Rabitz, 1989; Peirce *et al.*, 1991; Jakubetz *et al.*, 1990; Warren *et al.*, 1993; Yan *et al.*, 1993; Krause *et al.*, 1993; Kohler *et al.*, 1995).

This trial-and-error method is very time-consuming, requiring the repeated solution of the time-dependent Schrödinger equation. Further, by its very nature it often leads to solutions that provide little physical insight. When the explicit time-dependent terms in the Hamiltonian serve only to prepare a state that then evolves in the absence of an external field, or when its explicit time dependence can be treated adiabatically, there exists a more elegant method, called *coherent control* (CC) (Brumer and Shapiro, 1986; Shapiro and Brumer,

1987; Brumer and Shapiro, 1992; Shapiro and Brumer, 1993, 1997; Bandrauk *et al.*, 1992; Ivanov *et al.*, 1995; Muller *et al.*, 1990; Potvliege and Smith, 1992; Schafer and Kulander, 1992; Charron *et al.*, 1993), which requires the solution of the (time-independent) Schrödinger equation only once. Moreover, in that case, the CC solution allows for the simultaneous exploration of other possible future outcomes (and not just a single "desirable" objective), which results from different preparations of the initial wavefunction, provides physical insight into the nature of the control solution and provides analytic formulas for control that are useful experimentally. The coherent control method is the subject of the present review.

This review is organized as follows: Section II describes the basic principles behind the preparation and subsequent dynamics of a state excited by laser irradiation to the dissociative continuum. Section III then extends this approach to the excitation of a bound superposition state to show that quantum interference allows for control over dissociative dynamics. This idea, the principle of coherent control, is summarized in Section IV. Section V then describes a number of weak-field coherent control scenarios, including the demonstration that coherent control can be used to break symmetry and to generate chirality. In Section VI we introduce control methods in the strong-field limit, resulting in a powerful method (incoherent interference control) for the control of unimolecular processes. Section VII addresses the application of coherent control to collisional processes, and Section VIII provides a brief summary.

II. Preparation and Dynamics of a Continuum State

The desire to attain control over natural processes is of greatest significance if the control objectives involve *permanent* changes. Transitory objectives, which, once reached, exist only over a fleeting moment in time, are of academic interest but are of very little practical use. Thus, the types of systems we shall review here are those where events, such as bond breaking (dissociation), ionization, or particle exchange, take place over a small region in configuration space (the "interaction zone"). As the system departs from the interaction zone, its constituents decouple from one another and cease to change thereafter.

Under the above circumstances one is invariably dealing with *continuous* energy spectra. This is so because for bound states, which give rise to discrete spectra, decoupling at the end of the process is not possible. By its very definition, the constituents of a bound system remain close together at all times. Therefore, these constituents rarely reach a configuration where they decouple and cease to interact with one another.

Given that we are dealing with continuous spectra, the CC method utilizes some of the formal properties of the solutions of the multichannel scattering problem. In order to understand how and why these properties work, we first review the theory of the *coherent preparation* of an initial state composed of a continuum of scattering eigenfunctions.

Consider the case in which we prepare a wavepacket consisting of a superposition of scattering eigenstates $|E, \mathbf{m}^{\pm}\rangle$ of the material Hamiltonian, H_M, where

$$[E - H_M]|\, E, \mathbf{m}^{\pm}\rangle = 0 \tag{1}$$

subject to the normalization

$$\langle E', \mathbf{m}^{\pm}\, | E, \mathbf{n}^{\pm}\rangle = \delta(E - E')\delta_{\mathbf{m},\mathbf{n}} \tag{2}$$

Here E is the (continuous) energy and $\mathbf{m}$ designates all additional quantum numbers of relevance, e.g., the identity of the collision partners after the collision and all of the internal quantum numbers associated with each partner. The $\pm$ notation differentiates between *outgoing* (+) and *incoming* (−) boundary conditions (Levine, 1969), as explained in detail below.

As a specific method of preparation, we consider excitation of an initial bound state $|\, E_1\rangle$ by a laser pulse of the form

$$\epsilon(t) = \hat{\epsilon}\varepsilon(t) = \hat{\epsilon}\int_{-\infty}^{\infty} d\omega\, \bar{\epsilon}(\omega)\exp(-i\omega t) \tag{3}$$

where $\epsilon(t)$ is the pulse's electric field vector, $\hat{\epsilon}$ is the polarization direction, and $\bar{\epsilon}(\omega)$ is the Fourier transform of $\varepsilon(t)$ at angular frequency ω.

We wish to solve the time-dependent Schrödinger equation,

$$i\hbar\frac{d\Psi}{dt} = H\Psi \tag{4}$$

where H is the total Hamiltonian in the presence of the laser field,

$$H = H_M - \mathbf{d}\cdot\hat{\epsilon}\varepsilon(t) \tag{5}$$

with $\mathbf{d}$ being the transition-dipole operator and $\mathrm{d}\cdot\hat{\epsilon}$ its projection on the light's polarization direction. Assuming that the radiation-free eigenstates that predominate are the initial state $|\, E_1\rangle$ and a set of continuum states $|\, E, \mathbf{m}^{\pm}\rangle$,

we expand Ψ as

$$|\Psi(t)\rangle = b_1(t)|E_1\rangle \exp(-iE_1t/\hbar) + \sum_{n=1}^{N} \int dE b_{E,n}(t)|E,n^{\pm}\rangle \exp(-iEt/\hbar)$$
$$\equiv b_1(t)|E_1\rangle \exp(-iE_1t/\hbar) + |\Psi_e(t)\rangle \tag{6}$$

where $|\Psi_e(t)\rangle$, defined by Eq. (6), is the excited portion of the wavefunction (the "excited wavepacket").

In order to calculate b_1 and $b_{E,n}$ we substitute Eq. (6) in Eq. (4) to obtain a set of coupled first-order differential equations,

$$\frac{db_1(t)}{dt} = (i/\hbar) \sum_{n} \int dE b_{E,n}(t) \exp(-i\omega_{E,1}t)\varepsilon(t)\langle E_1|d\cdot\hat{\epsilon}|E,n^{\pm}\rangle$$
$$\frac{db_{E,m}(t)}{dt} = (i/\hbar) b_1(t) \exp(i\omega_{E,1}t)\varepsilon(t)\langle E,m^{\pm}|d\cdot\hat{\epsilon}|E_1\rangle \tag{7}$$

where $\omega_{E,1} \equiv (E - E_1)/\hbar$. In the presence of a sufficiently weak pulse, we can use first-order perturbation theory, according to which $b_1(t) \approx b_1(t=0) = 1$, and $b_{E,n}$ at the end of the pulse Eq. (7) is (Shapiro, 1993)

$$b_{E,n} = (2\pi i/\hbar)\bar{\varepsilon}(\omega_{E,1})\langle E,n^{\pm}|d\cdot\hat{\epsilon}|E_1\rangle \tag{8}$$

After the pulse is over, the excited wavepacket is therefore given as

$$|\Psi_e(t)\rangle = (2\pi i/\hbar) \sum_{n} \int dE \bar{\varepsilon}(\omega_{E,1})\langle E,n^{\pm}|d\cdot\hat{\epsilon}|E_1\rangle |E,n^{\pm}\rangle \exp(-iEt/\hbar) \tag{9}$$

We wish now to investigate the long-time properties of Eq. (9). To do so we need to relate the eigenstates of H_M to the eigenstates that describe the freely moving fragments at the end of the process. As an example, consider a triatomic molecule ABC, which breaks apart at the end of the process to yield the $A + BC$ channel (denoted $q = 1$) or the $B + AC$ channel (denoted $q = 2$). Below we explicitly discuss the formalism for the $A + BC$ product. However, the structure is the same for the $B + AC$ channel, with obvious substitutions in the equations.

The Hamiltonian H_M can be written as composed of three parts:

$$H_M = K_R + K_r + W(R,r) \tag{10}$$

Here $\mathbf{R}$ is the radius vector between A and the $B-C$ center of mass, $\mathbf{r}$ is the $B-C$ separation, $W(\mathbf{R},\mathbf{r})$ is the total potential energy of A, B, and C, and

$$K_{\mathbf{R}} = \frac{-\hbar^2}{2\mu}\nabla^2_{\mathbf{R}} \qquad K_{\mathbf{r}} = \frac{-\hbar^2}{2m}\nabla^2_{\mathbf{r}} \tag{11}$$

are the kinetic energy operators in $\mathbf{R}$ and $\mathbf{r}$, and μ and m are the reduced masses,

$$\mu = m_A(m_B+m_C)/(m_A+m_B+m_C), \qquad m = m_B m_C/(m_B+m_C) \tag{12}$$

If $v(r)$ denotes the asymptotic limit of $W(\mathbf{R},\mathbf{r})$ as A departs from $B-C$,

$$v(r) = \lim_{R\to\infty} W(\mathbf{R},\mathbf{r}) \tag{13}$$

it is clear that the $A-BC$ *interaction potential*, defined as

$$V(\mathbf{R},\mathbf{r}) \equiv W(\mathbf{R},\mathbf{r}) - v(r) \tag{14}$$

vanishes as $R\to\infty$, i.e., $\lim_{R\to\infty} V(\mathbf{R},\mathbf{r}) = 0$. Defining the $B-C$ Hamiltonian as

$$h_{\mathbf{r}} \equiv K_{\mathbf{r}} + v(r) \tag{15}$$

the triatomic Hamiltonian of Eq. (10) can now be rewritten, using Eq. (14), as

$$H_M = K_{\mathbf{R}} + h_{\mathbf{r}} + V(\mathbf{R},\mathbf{r}) \tag{16}$$

We see that it is the interaction potential $V(\mathbf{R},\mathbf{r})$ that couples the motion of the A atom to the motion of the BC diatomic. In its absence, the two free fragments A and BC described by the free Hamiltonian

$$H_0 \equiv K_{\mathbf{R}} + h_{\mathbf{r}} \tag{17}$$

move independently of one another. Because H_0 is a sum of two independent terms, its eigenstates, $|E,\mathbf{m};0\rangle$,

$$[E-H_0]|E,\mathbf{m};0\rangle = 0 \tag{18}$$

are given as products

$$|E,\mathbf{m};0\rangle = |e_{\mathbf{m}}\rangle|\mathbf{k}_{\mathbf{m}}\rangle \tag{19}$$

where

$$[e_{\mathbf{m}} - h_{\mathbf{r}}]|\, e_{\mathbf{m}}\rangle = 0 \tag{20}$$

with $e_{\mathbf{m}}$ being the *internal* (electronic, vibrational, rotational) energy of the $B - C$ diatomic and with $|\,\mathbf{k}_{\mathbf{m}}\rangle$ satisfying

$$[E - e_{\mathbf{m}} - K_{\mathbf{R}}]|\,\mathbf{k}_{\mathbf{m}}\rangle = 0 \tag{21}$$

describing the free (translational) motion of A relative to BC.

The solution of Eq. (21), written in the coordinate representation

$$\left[E - e_{\mathbf{m}} + \frac{\hbar^2}{2\mu}\nabla_{\mathbf{R}}^2\right]\langle \mathbf{R}|\,\mathbf{k}_{\mathbf{m}}\rangle = 0 \tag{22}$$

describes an energy-normalized plane wave of kinetic energy $E - e_{\mathbf{m}}$,

$$\langle \mathbf{R}|\,\mathbf{k}_{\mathbf{m}}\rangle = \left[\frac{\mathrm{m}k_{\mathbf{m}}}{\hbar^2(2\pi)^3}\right]^{1/2} \exp(i\mathbf{k}_{\mathbf{m}}\cdot\mathbf{R}) \tag{23}$$

where

$$k_m = \{2\mu(E - e_{\mathbf{m}})\}^{1/2}/\hbar \tag{24}$$

is the wavevector of the free motion of A relative to the BC center of mass. Because the free solutions assume the same continuous energy spectrum as do the full solutions $|\,E, \mathbf{n}^{\pm}\rangle$, they too satisfy the continuous spectrum normalization,

$$\langle E', \mathbf{m}; 0\,|E, \mathbf{n}; 0\rangle = \delta(E - E')\delta_{\mathbf{m},\mathbf{n}} \tag{25}$$

The eigenstates, $|\,E, \mathbf{n}^{\pm}\rangle$, of the fully interacting Hamiltonian H_M are related to $|\,E, \mathbf{n}; 0\rangle$ via the Lippmann-Schwinger equation (Taylor, 1972)

$$|\,E, \mathbf{n}^{\pm}\rangle = |\,E, \mathbf{n}; 0\rangle + \lim_{\epsilon\to 0}[E \pm i\epsilon - H_0]^{-1}V|\,E, \mathbf{n}^{\pm}\rangle \tag{26}$$

where the plus solution is known as the *outgoing* solution and the minus solution as the *incoming* solution. Each solution is an independent (though not mutually orthogonal) eigenstate of the full Schrödinger equation [Eq. (1)].

We now use the Lippmann-Schwinger equation to explore the long-time behavior of the wavepacket $\Psi_e(t)$ created with the laser pulse. Either the outgoing or the incoming set of solutions can be used as the basis set for expanding $\Psi_e(t)$. In what follows we shall see which type of solution is best for which purpose. Substituting Eq. (26) in Eq. (9), we obtain that

$$|\Psi_e(t)\rangle = (2\pi i/\hbar)\sum_{\mathbf{n}}\int dE \exp(-iEt/\hbar)\bar{\varepsilon}(\omega_{E,1})\langle E,\mathbf{n}^{\pm}|\mathbf{d}\cdot\hat{\epsilon}|E_1\rangle \{|E,\mathbf{n};0\rangle + [E\pm i\epsilon - H_0]^{-1}V|E,\mathbf{n}^{\pm}\rangle\} \tag{27}$$

Using the spectral resolution of $[E\pm i\epsilon - H_0]^{-1}$, we have from Eq. (27) that the probability amplitude of finding a free state $|E',\mathbf{m};0\rangle$ at time t is given as

$$\langle E',\mathbf{m};0|\Psi_e(t)\rangle = (2\pi i/\hbar)\sum_{\mathbf{n}}\int dE \exp(-iEt/\hbar)\bar{\varepsilon}(\omega_{E,1})\langle E,\mathbf{n}^{\pm}|\mathbf{d}\cdot\hat{\epsilon}|E_1\rangle \{\langle E'\mathbf{m};0|E,\mathbf{n};0\rangle + [E\pm i\epsilon - E']^{-1}\langle E'\mathbf{m};0|V|E,\mathbf{n}^{\pm}\rangle\} \tag{28}$$

Using the normalization of the free states [Eq. (25)], we have that

$$\langle E',\mathbf{m};0|\Psi_e(t)\rangle = (2\pi i/\hbar)\exp(-iE't/\hbar)\{\bar{\varepsilon}(\omega_{E',1})\langle E',\mathbf{m}^{\pm}|\mathbf{d}\cdot\hat{\epsilon}|E_1\rangle + \sum_{\mathbf{n}}\int dE \exp(-iEt/\hbar)\bar{\varepsilon}(\omega_{E,1})\langle E,\mathbf{n}^{\pm}|\mathbf{d}\cdot\hat{\epsilon}|E_1\rangle \times [E\pm i\epsilon - E']^{-1}\langle E'\mathbf{m};0|V|E,\mathbf{n}^{\pm}\rangle\} \tag{29}$$

In the $t\to\infty$ limit the integration over E can be performed analytically by contour integration. Note first that in that limit, the integrand on a large semicircle of radius R in the lower part of the complex E plane is zero, because when $E = Re^{i\theta}$, with $\theta < 0$,

$$\exp(-iEt/\hbar) = \exp(-iRe^{i\theta}t/\hbar) = \exp(-iR\cos\theta t/\hbar)\exp(R\sin\theta t/\hbar)_{t\to\infty}\to 0 \tag{30}$$

Thus, the result of the real E integration remains unchanged by supplementing it with integration along a large semicircle in the lower half E-plane. Because in the $-i\epsilon$ case, the integrand has a pole at $E = E' + i\epsilon$ that is outside the

closed contour, the whole integral is zero. We obtain that

$$\lim_{t\to\infty}\langle E',\mathbf{m};0\,|\Psi_e(t)\rangle = (2\pi i/\hbar)\bar{\varepsilon}(\omega_{E',1})\exp(-iE't/\hbar)\langle E',\mathbf{m}^-\,|\mathrm{d}\cdot\hat{\epsilon}|\,E_1\rangle \tag{31}$$

Hence the coefficients of expansion of the full wavepacket of Eq. (9), in terms of the $|\,E,\mathbf{m}^-\rangle$ states give the probability of observing states $|\,E,\mathbf{m};0\rangle$ in the distant future.

If instead of the incoming states we use the outgoing states, the closed-contour integration encircles a pole at $E = E' - i\epsilon$. Hence the integration yields

$$\lim_{t\to\infty}\langle E',\mathbf{m};0\,|\Psi_e(t)\rangle = (2\pi i/\hbar)\exp(-iE't/\hbar)\bar{\varepsilon}(\omega_{E',1}) \times\sum_{\mathbf{n}} S_{\mathbf{n},\mathbf{m}}(E')\langle E',\mathbf{n}^+\,|\mathrm{d}\cdot\hat{\epsilon}|\,E_1\rangle \tag{32}$$

where the $S_{\mathbf{n},\mathbf{m}}(E')$ matrix,

$$S_{\mathbf{n},\mathbf{m}}(E') \equiv \delta_{\mathbf{n},\mathbf{m}} - 2\pi i\langle E'\mathbf{m};0\,|V|\,E',\mathbf{n}^+\rangle \tag{33}$$

is known as the S-matrix or scattering matrix.

The form of Eq. (32) appears more complicated than that of Eq. (31) because each $\langle E,\mathbf{m};0\,|\Psi_e(t)\rangle$ component appears to be made up of contributions from all degenerate $|\,E,\mathbf{n};0\rangle$ states. Why use it at all then? The reason is that in ordinary scattering events, we want to use states whose past is well known to us. These are the outgoing states because when $t\to-\infty$, it is the contour on the semicircle in the upper half of the complex E-plane that vanishes. Supplementing the real-E integration by such a contour keeps the $E = E' - i\epsilon$ pole out of the contour, and we obtain that

$$\lim_{t\to-\infty}\langle E',\mathbf{m};0\,|\Psi_e(t)\rangle = (2\pi i/\hbar)\bar{\varepsilon}(\omega_{E',1})\exp(-iE't/\hbar)\langle E',\mathbf{m}^+\,|\mathrm{d}\cdot\hat{\epsilon}|\,E_1\rangle \tag{34}$$

In contrast, the $t\to-\infty$ limit appears more complicated with the incoming-states expansion because now the $E = E' + i\epsilon$ pole is enclosed by the contour, and we obtain that

$$\lim_{t\to-\infty}\langle E',\mathbf{m};0\,|\Psi_e(t)\rangle = (2\pi i/\hbar)\exp(-iE't/\hbar)\bar{\varepsilon}(\omega_{E',1}) \times\sum_{\mathbf{n}} S^-_{\mathbf{n},\mathbf{m}}(E')\langle E',\mathbf{n}^-\,|\mathrm{d}\cdot\hat{\epsilon}|\,E_1\rangle \tag{35}$$

where the $S^-_{\mathbf{n},\mathbf{m}}(E')$ matrix is defined as

$$S^-_{\mathbf{n},\mathbf{m}}(E') \equiv \delta_{\mathbf{n},\mathbf{m}} + 2\pi i \langle E'\mathbf{m}; 0 | V | E', \mathbf{n}^- \rangle \tag{36}$$

In the case of the optical pulse excitation, we use the incoming solutions because the origin of the system in the remote past is known to be $|E_1\rangle$ and our interest is in the fate of the system in the distant future.

III. Bichromatic Control of a Superposition State

Consider now how the laser field can be made to modify the outcome of the photo-dissociation process. As seen above, the probability of populating a "free" state $|e_\mathbf{m}\rangle|\mathbf{k}_\mathbf{m}\rangle$ at any given time is

$$P_\mathbf{m}(E)(t) = |\langle e_\mathbf{m} | \langle \mathbf{k}_\mathbf{m} | \Psi(t) \rangle|^2 \tag{37}$$

Using the expansion of $|\Psi(t)\rangle$ [Eq. (6)], we have that

$$\begin{aligned}\langle e_\mathbf{m} | \langle \mathbf{k}_\mathbf{m} | \Psi(t) \rangle = b_1(t) \langle e_\mathbf{m} | \langle \mathbf{k}_\mathbf{m} | E_1 \rangle \exp(-iE_1 t/\hbar) \\ + \sum_n \int dE b_{E,\mathbf{n}}(t) \langle e_\mathbf{m} | \langle \mathbf{k}_\mathbf{m} | E, \mathbf{n}^- \rangle \exp(-iEt/\hbar)\end{aligned} \tag{38}$$

Assuming that $\langle e_\mathbf{m} | E_1 \rangle = 0$, (e.g., the two states belong to different electronic states), it follows from Eq. (38) that in the long-time limit,

$$P_\mathbf{m}(E) = |\langle e_\mathbf{m} | \langle \mathbf{k}_\mathbf{m} | \Psi_e(t \to \infty) \rangle|^2 = |b_{E,\mathbf{m}}(t \to \infty)|^2 \tag{39}$$

Because

$$b_{E,\mathbf{n}}(t \to \infty) = \frac{i}{\hbar} \langle E, \mathbf{n}^- | \mathbf{d} \cdot \hat{\epsilon} | E_1 \rangle \int_{-\infty}^{\infty} dt' \varepsilon(t') \exp(-i\omega_{E,1} t) b_1(t') \tag{40}$$

it follows that

$$\frac{P_\mathbf{n}(E)}{P_\mathbf{m}(E)} = \left| \frac{b_{E,\mathbf{n}}(\infty)}{b_{E,\mathbf{m}}(\infty)} \right|^2 = \left| \frac{\langle E, \mathbf{n}^- | \mathbf{d} \cdot \hat{\epsilon} | E_1 \rangle}{\langle E, \mathbf{m}^- | \mathbf{d} \cdot \hat{\epsilon} | E_1 \rangle} \right|^2 \tag{41}$$

We see that the relative probabilities of populating different asymptotic states at a fixed energy E are *independent of the laser power and pulse shape*. This

result, which coincides with that of perturbation theory, holds true irrespective of the laser power, provided that only *one* initial state $|E_1\rangle$ is coupled to the continuum.

In order to affect the long-time outcome, we must therefore extend the treatment beyond the use of a single initial bound state. For example, starting from a linear superposition of two initial states

$$\Phi(t) = b_1|E_1\rangle \exp(-iE_1t/\hbar) + b_2|E_2\rangle \exp(-iE_2t/\hbar) \tag{42}$$

we have that

$$b_{E,\mathbf{n}}(t \to \infty) = \frac{i}{\hbar}\left\{\langle E,\mathbf{n}^-|\mathrm{d}\cdot\hat{\epsilon}|E_1\rangle\int_{-\infty}^{\infty} dt'\varepsilon(t')\exp(-i\omega_{E,1}t')b_1(t') + \langle E,\mathbf{n}^-|\mathrm{d}\cdot\hat{\epsilon}|E_2\rangle\int_{-\infty}^{\infty} dt'\varepsilon(t')\exp(-i\omega_{E,2}t')b_2(t')\right\} \tag{43}$$

In first-order perturbation theory, $b_1(t)$ and $b_2(t)$ are constant, so in the weak-field regime,

$$b_{E,\mathbf{n}}(t \to \infty) \approx \frac{2\pi i}{\hbar}\{\langle E,\mathbf{n}^-|\mathrm{d}\cdot\hat{\epsilon}|E_1\rangle\bar{\epsilon}(\omega_{E,1})b_1 + \langle E,\mathbf{n}^-|\mathrm{d}\cdot\hat{\epsilon}|E_2\rangle\bar{\epsilon}(\omega_{E,2})b_2\} \tag{44}$$

Recognizing that $\bar{\epsilon}(\omega)$ is complex, we can write

$$\bar{\epsilon}(\omega_{E,j}) = |\bar{\epsilon}(\omega_{E,j})|e^{-i\theta(\omega_{E,j})}, \quad (j = 1,2) \tag{45}$$

and transform Eq. (44) into

$$b_{E,\mathbf{n}}(\infty) = \frac{2\pi i}{\hbar}\{\langle E,\mathbf{n}^-|\mathrm{d}\cdot\hat{\epsilon}|E_1\rangle|\bar{\epsilon}(\omega_{E,1})|e^{-i\theta(\omega_{E,1})}b_1 + \langle E,\mathbf{n}^-|\mathrm{d}\cdot\hat{\epsilon}|E_2\rangle|\bar{\epsilon}(\omega_{E,2})|e^{-i\theta(\omega_{E,2})}b_2\} \tag{46}$$

Then, the probability of observing product state $\mathbf{n}$ at infinite time is given as,

$$P_{\mathbf{n}}(E) = \frac{4\pi^2}{\hbar^2}|\langle E,\mathbf{n}^-|\mathrm{d}\cdot\hat{\epsilon}|E_1\rangle|\bar{\epsilon}(\omega_{E,1})|e^{-i\theta(\omega_{E,1})}b_1 + \langle E,\mathbf{n}^-|\mathrm{d}\cdot\hat{\epsilon}|E_2\rangle|\bar{\epsilon}(\omega_{E,2})|e^{-i\theta(\omega_{E,2})}b_2|^2 \tag{47}$$

We see that the pulse attributes have been "imprinted" onto the material matrix elements. As a result, by changing the pulse attributes, we *can* change the branching ratios into different product channels.

The properties we wish to control are often the branching ratios to different chemical products. Note, however, that the approach advocated below, and indeed any CC scenario, can be readily modified to control probabilities of populating individual product states. Realizing that any chemical process such as

$$A + BC(\mathbf{n}) \xleftarrow{q=1} ABC \xrightarrow{q=2} AB(\mathbf{n}) + C \tag{48}$$

involves a multitude of internal fragment states ($|e_{\mathbf{n}}\rangle$) in each chemical channel, we calculate the total probability to produce products in one of the q channels as

$$P^{(q)}(E) = \sum_{\mathbf{n}} P^{(q)}_{\mathbf{n}}(E) = \sum_{\mathbf{n}} \frac{4\pi^2}{\hbar^2} |\langle E, q, \mathbf{n}^- | \mathrm{d} \cdot \hat{\epsilon} | E_1 \rangle \bar{\epsilon}(\omega_{E,1}) | e^{-i\theta(\omega_{E,1})} b_1 + \langle E, q, \mathbf{n}^- | \mathrm{d} \cdot \hat{\epsilon} | E_2 \rangle \bar{\epsilon}(\omega_{E,2}) | e^{-i\theta(\omega_{E,1})} b_2 |^2 \tag{49}$$

Here we have modified our notation so that $\mathbf{n}$ denotes all quantum numbers other than the arrangement channel label q. By expanding the square, the above expression transforms to

$$P^{(q)}(E) = P^{(q)}_{11}(E) + P^{(q)}_{22}(E) + P^{(q)}_{12}(E) \tag{50}$$

where

$$P^{(q)}_{jj}(E) = \frac{4\pi^2}{\hbar^2} \mu^{(q)}_{jj} |\bar{\epsilon}(\omega_{E,j}|^2 b_j^2 \quad (j = 1,2)$$
$$P^{(q)}_{12}(E) = \frac{4\pi^2}{\hbar^2} |\bar{\epsilon}(\omega_{E,1})| |\bar{\epsilon}(\omega_{E,2})| 2\mathcal{R}_e\{\mu^{(q)}_{12} e^{-i\theta_{12}} b_1^* b_2\} \tag{51}$$

where

$$\mu^{(q)}_{jj} \equiv \sum_{\mathbf{n}} |\langle E, q, \mathbf{n}^- | \mathrm{d} \cdot \hat{\epsilon} | E_j \rangle|^2, \quad (j = 1,2)$$
$$\mu^{(q)}_{12} = \sum_{\mathbf{n}} \langle E_1 | \mathrm{d} \cdot \hat{\epsilon} | E, q, \mathbf{n}^- \rangle \langle E, q, \mathbf{n}^- | \mathrm{d} \cdot \hat{\epsilon} | E_2 \rangle \tag{52}$$

and $\theta_{12} \equiv \theta(\omega_{E,2}) - \theta(\omega_{E,1})$.

The $P_{11}^{(q)}(E)$ and $P_{22}^{(q)}(E)$ terms are the probabilities of photo-dissociating levels $|E_1\rangle$ and $|E_2\rangle$, respectively. The $P_{12}^{(q)}(E)$ is the interference term. It is the only term influenced by the relative phase θ_{12} between the $\bar{\epsilon}(\omega_{E,1})$ and $\bar{\epsilon}(\omega_{E,2})$ field modes.

In order to make the structure of the probability expression Eq. (51) clearer, we write the complex amplitude $\mu_{12}^{(q)}$ as

$$\mu_{12}^{(q)} = |\mu_{12}^{(q)}| e^{i\phi_{12}^{(q)}} \tag{53}$$

where $\phi_{12}^{(q)}$ is the so-called "molecular" or "material" phase, and define the phase α_{12} via

$$b_1^* b_2 = |b_1 b_2| e^{-i\alpha_{12}} \tag{54}$$

With these definitions, the interference term assumes the form

$$P_{12}^{(q)}(E) = \frac{8\pi^2}{\hbar^2} |\bar{\epsilon}(\omega_{E,1})\bar{\epsilon}(\omega_{E,2})\mu_{12}^{(q)} b_1 b_2| \cos[\phi_{12}^{(q)} - \alpha_{12} - \theta_{12}] \tag{55}$$

Because of the dependence of $\phi_{12}^{(q)}$ on q, this term can be positive ("constructive interference") or negative ("destructive interference") with respect to one q channel and the opposite with respect to the other. Hence, by tuning the external phases α_{12} or θ_{12}, we can make the sign of this term negative with respect to one q chemical channel and positive with respect to another. In this way, by changing an external phase factor that is indifferent to the final channels, we attain selectivity (discrimination) between the final channels. The magnitude of this effect can be enhanced by varying the ratio

$$x \equiv \frac{|\bar{\epsilon}(\omega_{E,1}) b_1|}{|\bar{\epsilon}(\omega_{E,2}) b_2|}$$

The method of controlling the final outcome of a process in this way is at the heart of coherent control.

The structure of the CC equations is most transparent when we write Eq. (50) and Eq. (51) as

$$P^{(q)}(E) = \frac{4\pi^2}{\hbar^2} |\bar{\epsilon}(\omega_{E,1}) b_1|^2 \{\mu_{11}^{(q)} + x^2 \mu_{22}^{(q)} + 2x|\mu_{12}^{(q)}| \cos[\phi_{12}^{(q)} - \alpha_{12} - \theta_{12}]\} \tag{56}$$

In order to attain maximum control over $R_{q'q}$, we can set $P^{(q)}(E) = 0$ for one of the q channels. Both $P^{(q)}(E)$ and $\mu_{11}^{(q)} + x^2\mu_{22}^{(q)}$ of Eq. (56) are positive, so the only way we can minimize $P^{(q)}(E)$ is by making the interference term $2x|\mu_{12}^{(q)}|\cos[\phi_{12}^{(q)} - \alpha_{12} - \theta_{12}]$ as negative as possible, which means setting the external phases such that

$$\alpha_{12} + \theta_{12} = \pi - \phi_{12}^{(q)} \tag{57}$$

Under these circumstances, $\cos[\phi_{12}^{(q)} - \alpha_{12} - \theta_{12}] = -1$ and Eq. (56) becomes

$$P^{(q)}(E) = \frac{4\pi^2}{\hbar^2}|\bar{\epsilon}(\omega_{E,1})b_1|^2\{\mu_{11}^{(q)} + x^2\mu_{22}^{(q)} - 2x|\mu_{12}^{(q)}|\} = 0 \tag{58}$$

This is a quadratic equation in x that has a solution $x = |\mu_{12}^{(q)}|/\mu_{22}^{(q)}$, if and only if $|\mu_{12}^{(q)}|^2 = \mu_{11}^{(q)}\mu_{22}^{(q)}$.

In order to see the circumstances under which this condition is fulfilled we write,

$$\begin{aligned}
\mu_{11}^{(q)} &= \sum_{\mathbf{n}} \langle E_1 |\mathrm{d}\cdot\hat{\epsilon}| E, q, \mathbf{n}^-\rangle\langle E, q, \mathbf{n}^-|\mathrm{d}\cdot\hat{\epsilon}|E_1\rangle \\
&= \langle E_1|\mathrm{d}\cdot\hat{\epsilon}\left\{\sum_{\mathbf{n}}|E, q, \mathbf{n}^-\rangle\langle E, q, \mathbf{n}^-|\right\}\mathrm{d}\cdot\hat{\epsilon}|E_1\rangle = \langle E_1\mathrm{d}\cdot\hat{\epsilon}P|P\mathrm{d}\cdot\hat{\epsilon}E_1\rangle \\
\mu_{22}^{(q)} &= \sum_{\mathbf{n}} \langle E_2 |\mathrm{d}\cdot\hat{\epsilon}| E, q, \mathbf{n}^-\rangle\langle E, q, \mathbf{n}^-|\mathrm{d}\cdot\hat{\epsilon}|E_2\rangle = \langle E_2\mathrm{d}\cdot\hat{\epsilon}P|P\mathrm{d}\cdot\hat{\epsilon}E_2\rangle \\
|\mu_{12}^{(q)}| &= \left|\sum_{\mathbf{n}} \langle E_1 |\mathrm{d}\cdot\hat{\epsilon}| E, q, \mathbf{n}^-\rangle\langle E, q, \mathbf{n}^-|\mathrm{d}\cdot\hat{\epsilon}|E_2\rangle\right| = |\langle E_1\mathrm{d}\cdot\hat{\epsilon}P|P\mathrm{d}\cdot\hat{\epsilon}E_2\rangle|
\end{aligned} \tag{59}$$

where

$$P \equiv \sum_{\mathbf{n}} |E, q, \mathbf{n}^-\rangle\langle E, q, \mathbf{n}^-| \tag{60}$$

and we have used the fact that the projection operator P satisfies $PP = P$. Hence the $\mu_{11}^{(q)}$, $\mu_{22}^{(q)}$, and $|\mu_{12}^{(q)}|$ matrix elements are related as scalar products of the $|E_1\mathrm{d}\cdot\hat{\epsilon}P\rangle$ and $|P\mathrm{d}\cdot\hat{\epsilon}E_2\rangle$ state vectors. By the Schwarz inequality,

$$|\langle E_1\mathrm{d}\cdot\hat{\epsilon}P|P\mathrm{d}\cdot\hat{\epsilon}E_2\rangle|^2 \leq \langle E_1\mathrm{d}\cdot\hat{\epsilon}P|P\mathrm{d}\cdot\hat{\epsilon}E_1\rangle\langle E_2\mathrm{d}\cdot\hat{\epsilon}P|P\mathrm{d}\cdot\hat{\epsilon}E_2\rangle \tag{61}$$

with the equality holding only when $|E_1 \mathrm{d}\cdot\hat{\epsilon}P\rangle$ and $|P\mathrm{d}\cdot\hat{\epsilon}E_2\rangle$ are parallel to one another. If P is a projection onto a single state — i.e., no $\mathbf{n}$ summation need be performed — then the equality in Eq. (61) holds. That is, by definition, the case, because by definition,

$$\begin{aligned}&|\langle E_1 \mathrm{d}\cdot\hat{\epsilon}|\,E,q^-\rangle\langle E,q^-|\mathrm{d}\cdot\hat{\epsilon}E_2\rangle|^2\\&\quad=\langle E_1\mathrm{d}\cdot\hat{\epsilon}|\,E,q^-\rangle\langle E,q,^-|\mathrm{d}\cdot\hat{\epsilon}E_1\rangle\langle E_2\mathrm{d}\cdot\hat{\epsilon}|\,E,q^-\rangle\langle E,q^-|\mathrm{d}\cdot\hat{\epsilon}E_2\rangle\end{aligned}$$

In all other cases, because of the existence of many $\mathbf{n}$ internal states, the strict inequality holds and the solution of Eq. (58) can never be realized. Nevertheless, numerous computational studies, some discussed below, show that control is extensive.

In general, experiments measure energy-averaged quantities such as the probability P_q of forming product in channel q, and the ratio $R_{q,q'}$ of product in each channel:

$$\begin{aligned}P_q&=\int dE\,P_q(E)\\R_{q,q'}&=P_q/P_{q'}\end{aligned}\tag{62}$$

because products are not distinguished on the basis of total energy. For the case considered above, the photo-dissociation of a superposition state, $P_q(E)$ is nonzero at three energies: $E=E_1+\hbar\omega_{E,1}=E_2+\hbar\omega_{E,2}, E=E_1+\hbar\omega_{E,2}$, and $E=E_2+\hbar\omega_{E,1}$. The contribution from the first of these energies, $P_q(E=E_1+\hbar\omega_{E,1})$, is given in Eq. (49), where the remaining contributions are

$$\begin{aligned}P_q(E=E_1+\hbar\omega_{E,2})&=\left(\frac{2\pi}{\hbar}\right)^2|b_1\bar{\epsilon}(\omega_{E,2})|^2\mu_q(11)\\P_q(E=E_2+\hbar\omega_{E,1})&=\left(\frac{2\pi}{\hbar}\right)^2|b_2\bar{\epsilon}(\omega_{E,1})|^2\mu_q(22)\end{aligned}\tag{63}$$

Thus, the overall P_q for $N=2$ is given by

$$P_q=P_q(E=E_1+\hbar\omega_{E,1})+P_q(E=E_1+\hbar\omega_{E,2})+P_q(E=E_2+\hbar\omega_{E,1})\tag{64}$$

The latter two terms correspond to traditional photo-dissociation terms without associated interference contributions and provide *uncontrollable* photo-dissociation terms that we call "satellites." In this and all coherent

control scenarios discussed below, it is important to attempt to reduce the relative magnitude of the satellite terms in order to increase overall controllability.

As the first example of coherent control, consider the bichromatic control of the photo-dissociation of methyl iodide in the A band (near 266 nm):

$$CH_3 + I^*(^2P_{1/2}) \leftarrow CH_3I \rightarrow CH_3 + I(^2P_{3/2}) \tag{65}$$

The control objective is the formation of ground-state iodine [$I(^2P_{3/2})$, denoted I] versus excited-state iodine [$I(^2P_{1/2})$, denoted I*]. The computation considered a rotating collinear model in which the H_3 center of mass, the C, and the I groups are assumed to lie on a line (Shapiro and Brumer, 1987). All satellite terms are included. The bound states $|E_i\rangle$ are characterized in this case by v, J, and M_J, the vibrational, rotational, and magnetic quantum numbers. Figure 1 shows contour plots of the yield of $CH_3 + I^*$ (i.e., the fraction of product that is $CH_3 + I^*$), as a function of θ_{12} and $s = x^2/[1 + x^2]$ in the photo-dissociation of CH_3I out of an equal superposition of the $|v_1 = 0, J_1 = 2\rangle$ and $|v_2 = 1, J_2 = 2\rangle$ states at two different frequencies, $\omega_{E,1} = 39{,}639\,\text{cm}^{-1}$ and $\omega_{E,1} = 42{,}367\,\text{cm}^{-1}$. The M_J magnetic quantum number is averaged over, and all satellite terms are included. Clearly, control is extensive, ranging from 0.3 to 0.75 as the control parameters are varied. Note also that a comparison of Figs. 1(a) and 1(b), which correspond to results at different excitation frequencies, shows that there is considerable dependence of the control contour topology on frequency.

This bichromatic scenario has been extended theoretically in a number of ways. For example, we have considered (Shapiro and Brumer, 1992) the extension of this scenario to a superposition of N bound states excited by N laser frequencies and demonstrated total control over the dynamics under certain conditions. We have also considered the two-level approach in the condensed phase (Shapiro and Brumer, 1989) in order to examine the effect of collisions and dephasing on control. In particular, the CC scenario described above was extended in the following way. The initial superposition state [Eq. (42)] was assumed prepared by two-photon absorption in the presence of collisions, modeled by a Bloch equation with appropriate T_1, T_2 relaxation times. This transition was assumed saturated, establishing a time-independent density matrix describing this two-level system. This superposition was then pumped to dissociation by a pulsed laser whose width exceeds the spacing between the pair of bound levels. Thus, the pump laser contains both frequencies $\omega_{E,1}, \omega_{E,2}$ necessary to excite the superposition to the same continuum energy E. The resultant branching in CH_3I [Eq. (65)] was examined, and control was found to survive over a substantial temperature range. This model computation motivates applications of CC in the condensed phase, as do the experiments discussed in Section VIII.

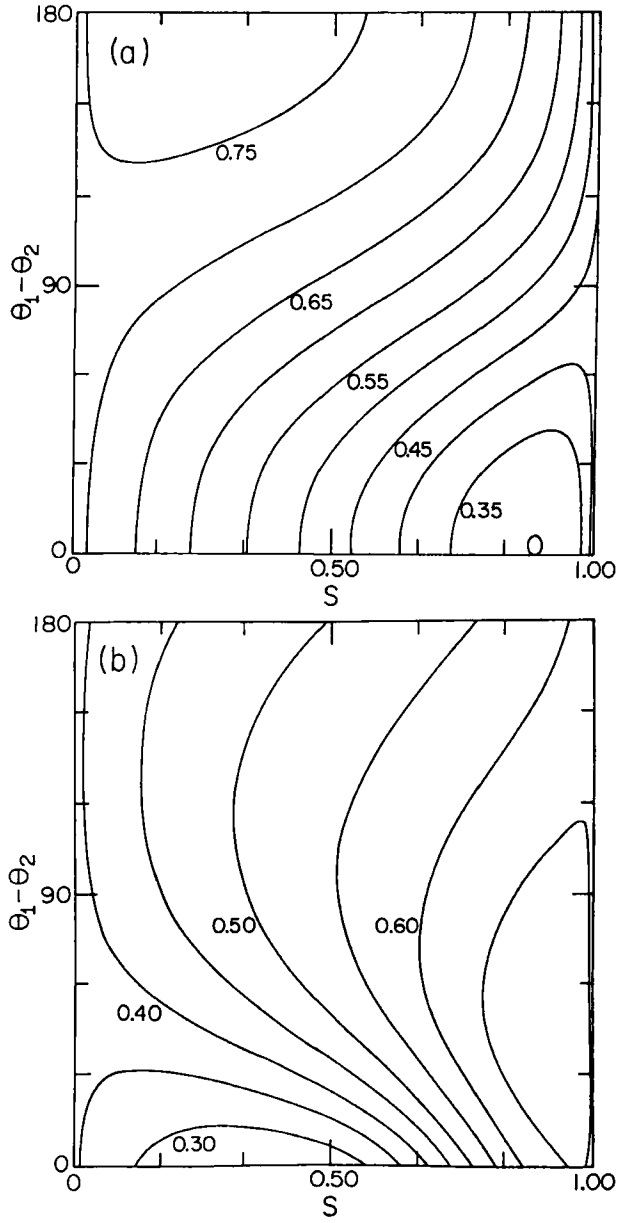

FIG. 1. Contour plot of the yield of I^* (i.e., fraction of I^* as product) in the bichromatically controlled photo-dissociation of CH_3I starting from an M-averaged initial state. (a) $\omega_{E,1} = 39{,}639\,\mathrm{cm}^{-1}$, (b) $\omega_{E,1} = 42{,}367\,\mathrm{cm}^{-1}$. (From Shapiro and Brumer, 1987.)

IV. The Coherent Control Principle

Photo-dissociation of a superposition state, the scenario described above, will be seen to be just one particular implementation of a general principle of coherent control, i.e., that *coherently driving a state with phase coherence through multiple optical excitation routes to the same final state allows for the possibility of control.* This procedure has a well-known analogy: the interference between paths as a beam of either particles or light passes through a double slit. In that case, interference between two coherent beams leads to spatial patterns of enhanced or reduced probabilities on an observation screen. In the case of coherent control, the overall coherence of a pure state plus laser source allows for the constructive or destructive manipulation of probabilities in product channels. Active control results because the excitation process explicitly imparts experimentally controllable phase and amplitude information to the molecule.

It is important to note that, in general, quantum-interference-based control occurs only between energetically degenerate states. To see this, note that if the excitation creates product states of energy E and E', then the interference term [e.g., Eq. (55)] would carry the phase $\exp[i(E - E')t/\hbar]$. Thus, this term, as well as the interference term, would average to zero over a small time interval, and control would be lost.

Further, it is worth noting that CC scenarios often lead to simple analytic expressions for reaction probabilities in terms of a few molecular parameters and a few control parameters. Hence, the entire dependence of product probabilities on the control parameters can be easily generated experimentally once the molecular terms are determined from a fit of the control expression to a small number of experimentally determined yields.

Numerous scenarios can be designed that rely on the essential coherent control principle. Several are discussed in the following sections.

V. Weak-Field Coherent Control: Unimolecular Processes

A. Interference Between N-Photon and M-Photon Routes

Rather than starting with a nonstationary superposition state, as above, we can achieve CC by photo-dissociating a *single* stationary state via two optical paths (Shapiro *et al.*, 1988). Such paths can consist, for example, of an N-photon process and an M-photon process satisfying $N\omega_N = M\omega_M$, with ω_N and ω_M being the optical frequencies of each path. The numbers N and M can be of the same parity or of opposite parity. It turns out that the latter allows for control over the photo-dissociation differential cross sections, whereas the former

allows for control over both the integral and the differential cross sections. For simplicity we focus here on the three lowest-order cases $(N,M)=(1,3)$, $(N,M)=(1,2)$, and $(N,M)=(2,2)$. Other cases, such as the $(N,M)=(2,4)$ case (Bandrauk *et al.*, 1992; Chelkowski and Bandrauk, 1991), and strong-field extensions (Charron *et al.*, 1995; Szöke *et al.*, 1991; Zuo and Bandrauk, 1996) have been discussed in the literature.

1. One-Photon versus Three-Photon Interference

We consider (Shapiro *et al.*, 1988) a molecule, initially in state $|g\rangle|E_i\rangle$, where $|g\rangle$ denotes the ground electronic state, subjected to two co-propagating CW fields of frequencies ω_1 and ω_3 with $\omega_3 = 3\omega_1$. The total Hamiltonian is given by

$$H = H_M - 2\mathbf{d}\cdot\mathcal{R}_e[\hat{\epsilon}_3\bar{\epsilon}_3\exp(-i\omega_3 t) + \hat{\epsilon}_1\bar{\epsilon}_1\exp(-i\omega_1 t)] \tag{66}$$

where $\bar{\epsilon}_i \equiv \bar{\epsilon}(\omega_i)$.

We assume the following physics: (a) dipole transitions within electronic states are negligible compared to those between electronic states; (b) the fields are sufficiently weak to allow the use of perturbation theory; and (c) $E_i + 2\hbar\omega_1$ is below the dissociation threshold, with dissociation occurring in the $|e\rangle$-excited electronic manifold.

Given the above assumptions, the lowest-order expression for the one-photon or three-photon dissociation amplitude $A_{q,\mathbf{m}}(E = E_i + \hbar\omega_1)$ is

$$\begin{aligned} A_{q,\mathbf{m}}(E = E_i + \hbar\omega_1) = \left(\frac{2\pi i}{\hbar}\right)[&\delta(\omega_3 - \omega_{E,i})\bar{\epsilon}_3\langle E,q,\mathbf{m}^-\,|\,\mathrm{d}_{e,g}\,|\,E_i\rangle \\ &+ \delta(3\omega_1 - \omega_{E,i})\bar{\epsilon}_1^3\langle E,q,\mathbf{m}^-\,|\,T\,|\,E_i\rangle] \end{aligned} \tag{67}$$

where $\mathrm{d}_{e,g} \equiv \langle e\,|\mathrm{d}\cdot\hat{\epsilon}|\,g\rangle$ and T denotes the three-photon transition operator, given in third-order perturbation theory as

$$T = \mathrm{d}_{e,g}(E_i - H_g + 2\hbar\omega_1)^{-1}\mathrm{d}_{g,e}(E_i - H_e + \hbar\omega_1)^{-1}\mathrm{d}_{e,g} \tag{68}$$

Because all light sources have a finite frequency width, we can integrate over this width to obtain

$$P_q(E) = \sum_{\mathbf{m}}\left|\int d\omega_3 A_{q,\mathbf{m}}(E = E_i + \hbar\omega_1)\right|^2 = P_q^{(1)}(E) + P_q^{(3)}(E) + P_q^{(13)}(E) \tag{69}$$

where the one-photon photodissociation probability is

$$P_q^{(1)}(E) = \left(\frac{2\pi}{\hbar}\right)^2 |\bar{\epsilon}_3|^2 \sum_{\mathbf{m}} |\langle E, q, \mathbf{m}^- \,|\, \mathrm{d}_{e,g} \,|\, E_i\rangle|^2 \tag{70}$$

the three-photon photodissociation probability is

$$P_q^{(3)}(E) = \left(\frac{2\pi}{\hbar}\right)^2 |\bar{\epsilon}_1|^6 \sum_{\mathbf{m}} |\langle E, q, \mathbf{m}^- \,|\, T \,|\, E_i\rangle|^2 \tag{71}$$

and the one-photon/three-photon interference term is

$$P_q^{(13)}(E) = \left(\frac{2\pi}{\hbar}\right)^2 \left[\bar{\epsilon}_3 \bar{\epsilon}_1^3 \sum_{\mathbf{m}} \langle E_i \,|\, T \,|\, E, q, \mathbf{m}^-\rangle \langle E, q, \mathbf{m}^- \,|\, \mathrm{d}_{e,g} \,|\, E_i\rangle + c.c.\right] \tag{72}$$

As in our discussion of the photo-dissociation of a superposition state, we define a "molecular" interference-amplitude $|F_q^{(13)}|$ and a "molecular" phase $\delta_q^{(13)}$ as

$$|F_q^{(13)}| \exp(i\delta_q^{(13)}) \equiv \sum_{\mathbf{m}} \langle E_i \,|\, T \,|\, E, q, \mathbf{m}^-\rangle \langle E, q, \mathbf{m}^- \,|\, \mathrm{d}_{e,g} \,|\, E_i\rangle \tag{73}$$

Recognizing that $\bar{\epsilon}_i$ may be complex, $\bar{\epsilon}_i = |\bar{\epsilon}_i| e^{i\phi_i}$, we can write the above interference term as

$$P_q^{(13)}(E) = -2\left(\frac{2\pi}{\hbar}\right)^2 |\bar{\epsilon}_3 \bar{\epsilon}_1^3| \cos(\phi_3 - 3\phi_1 + \delta_q^{(13)}) |F_q^{(13)}| \tag{74}$$

The branching ratio $R_{qq'}(E)$ for channels q and q' can then be written as

$$R_{qq'}(E) = \frac{F_q^{(1)} - 2x\cos(\phi_3 - 3\phi_1 + \delta_q^{(13)})\epsilon_0^2 |F_q^{(13)}| + x^2 \epsilon_0^4 F_q^{(3)}}{F_{q'}^{(1)} - 2x\cos(\phi_3 - 3\phi_1 + \delta_{q'}^{(13)})\epsilon_0^2 |F_{q'}^{(13)}| + x^2 \epsilon_0^4 F_{q'}^{(3)}} \tag{75}$$

where

$$F_q^{(1)} = \left(\frac{\hbar}{\pi|\bar{\epsilon}_3|}\right)^2 P_q^{(1)}(E); \quad F_q^{(3)} = \left(\frac{\hbar}{\pi|\bar{\epsilon}_1|^3}\right)^2 P_q^{(3)}(E) \tag{76}$$

and

$$x = \frac{|\bar{\epsilon}_1|^3}{\epsilon_0^2 |\bar{\epsilon}_3|} \tag{77}$$

where ϵ_0 is defined as a single unit of electric field. x is therefore a dimensionless parameter.

The numerator and denominator of Eq. (75) both display the canonical form for coherent control, i.e., a form similar to Eq. (50) in which there are independent contributions from more than one route, modulated by an interference term. Because the interference term is controllable through variation of laboratory parameters, so too is the product ratio $R_{qq'}(E)$. Thus, the principle on which this control scenario is based is the same as that in Section III, but the interference is introduced in an entirely different way.

With the qualitative principle of interfering pathways exposed, we demonstrate the quantitative extent to which the one-photon versus three-photon scenario alters the yield ratio in a realistic system by considering the photodissociation of IBr:

$$\mathrm{I} + \mathrm{Br} \leftarrow \mathrm{IBr} \rightarrow \mathrm{I} + \mathrm{Br}^* \tag{78}$$

where $\mathrm{Br} = \mathrm{Br}(^2P_{3/2})$ and $\mathrm{Br}^* = \mathrm{Br}(^2P_{1/2})$. Reliable IBr potential curves were used throughout the calculation.

Computational results on this system were obtained (Chan *et al.*, 1991) for two different cases: excitation from states of fixed M_i (the projection of the diatomic angular momentum J_i along the z-axis) and for the average over initial M_i. Results, in the form of a contour plot of the Br^* yield for excitation from $v = 0, J_i = 1, M_i = 0$, and $J_i = 42$ (M_i averaged) are shown in Figs. 2 and 3 as a function of $s = x^2/(1 + x^2)$ and of the relative laser phase $(\phi_3 - 3\phi_1)$. The range of control in each case is impressive, with essentially no loss of control due to M averaging.

The three-photon versus one-photon scenario has been experimentally realized in atoms (Chen *et al.*, 1990) and by Gordon and coworkers (Park *et al.*, 1991; Lu *et al.*, 1992; Kleiman *et al.*, 1995; Zhu *et al.*, 1995, 1997) in a series of experiments on HCl, H_2S, and CO. In the case of HCl, the molecule was excited to an intermediate $^3\Sigma^-(\Omega^+)$ vib-rotational resonance, using a combination of three ω_1 ($\lambda_1 = 336\,\mathrm{nm}$) photons and one ω_3 ($\lambda_3 = 112\,\mathrm{nm}$) photon. The ω_3 beam was generated from an ω_1 beam by tripling in a Kr gas cell. Ionization of the intermediate state takes place by absorption of one additional ω_1 photon. Similar demonstrations in ammonia, trimethylamine, triethylamine, cyclooctatetraene, and 1,1-dimethylhydrazine have been reported by Bersohn and coworkers (Wang *et al.*, 1996b) and in Na by Cavalieri *et al.* (1997). Later

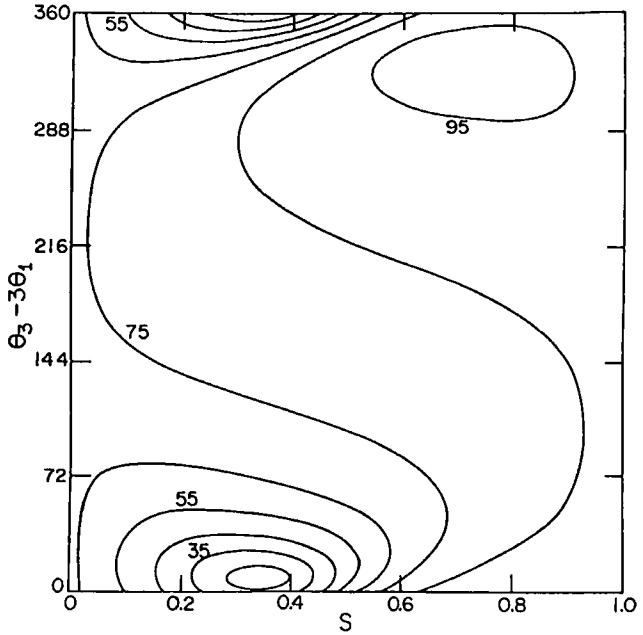

FIG. 2. Contour plot of the yield of Br* (percentage of Br* as product) in the photodissociation of IBr by the one-photon versus three-photon scenario. The abscissa is the amplitude parameter $s = x^2/(1+x^2)$, and the ordinate is $\theta_3 - 3\theta_1$. Here $\omega_1 = 6657.5\,\text{cm}^{-1}$. (From Chan *et al.*, 1991).

studies (Zhu *et al.*, 1995, 1997) demonstrated control over the production of different channels, specifically the HI^+ versus the H + I channels, in the photoexcitation of HI. This result is highly significant, showing the ability to control the *relative* yield of products in photo-dissociation.

In all of these experiments, control over $R_{qq'}(E)$ was obtained by varying the phase difference $(\phi_3 - 3\phi_1)$ and the parameter x. In doing so, the experiments used co-propagating ω_1 and ω_3 beams with wavevectors suitably "phase-matched" so that Eq. (75) no longer contains the spatial coordinate z, and the interference term is independent of the position in space.

It is also possible to use the one-photon versus three-photon (indeed any N-photon versus M-photon) control scenario to control differential cross sections. To see this, consider rewriting Eqs. (70) through (73) so that they apply to the probability of observing the product in channel q, but at a fixed scattering angle. Then the sum on $\mathbf{m}$ no longer includes an integral over scattering angles. The resultant interference term $P_q^{(13)}$ is nonzero, so varying the properties of the lasers will indeed alter the differential cross section into channel q.

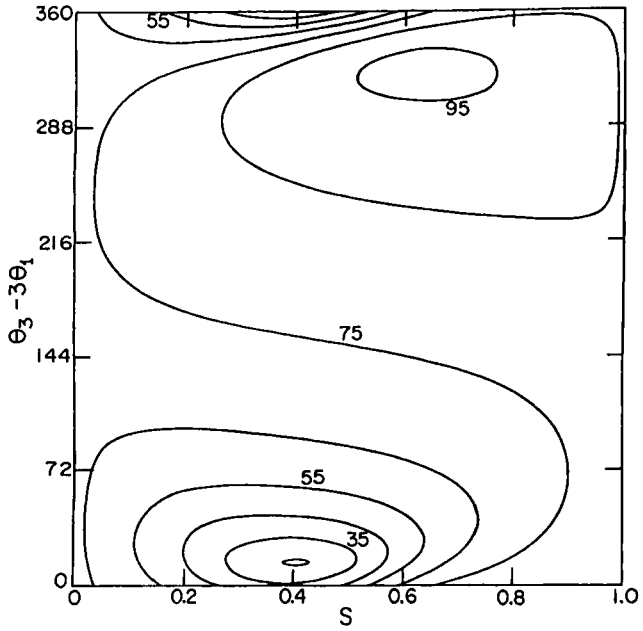

FIG. 3. As in Fig. 2 but for $v = 0$, $J_i = 42$, $\omega_1 = 6635.0\,\mathrm{cm}^{-1}$ with an average over initial M_J. (From Chan *et al.*, 1991.)

2. *One-Photon versus Two-Photon Interference*

Although scenarios for simultaneous absorption of N plus M photons, where N, M are of the same parity, allow for control over both the differential and integral photo-dissociation cross sections, this is not the case when N, M are of different parity. In this case, only control over the differential cross section is possible. To see this, we consider the case of simultaneous one-photon versus two-photon absorption.

The Hamiltonian for a molecule irradiated with two frequencies ω_1 and ω_2, with $\omega_2 = 2\omega_1$, is

$$H = H_M - 2\mathbf{d} \cdot \mathcal{R}_e[\hat{\epsilon}_2 \bar{\epsilon}_2 \exp(-i\omega_2 t) + \hat{\epsilon}_1 \bar{\epsilon}_1 \exp(-i\omega_1 t)] \tag{79}$$

Assuming that $E_i + \hbar\omega_1$ is below the threshold for photo-dissociation and that absorption of ω_1 is via an intermediate electronic state that is dipole accessible, we obtain, in complete analogy to the one-photon versus three-photon case, that the probability $P_q(E, \hat{\mathbf{k}})$ of photo-dissociation into channel q at recoil angles $\hat{\mathbf{k}} \equiv (\theta_k, \phi_k)$ is given by

$$P_q(E, \hat{\mathbf{k}}) = P_q^{(1)}(E, \hat{\mathbf{k}}) + P_q^{(12)}(E, \hat{\mathbf{k}}) + P_q^{(2)}(E, \hat{\mathbf{k}}) \tag{80}$$

where

$$P_q^{(1)}(E,\hat{\mathbf{k}}) = \left(\frac{2\pi}{\hbar}\right)^2 |\bar{\epsilon}_2|^2 |\langle E,\hat{\mathbf{k}},q^- \,|\, \mathrm{d}_{e,g} \,|\, E_i\rangle|^2 \tag{81}$$

$$P_q^{(2)}(E,\hat{\mathbf{k}}) = \left(\frac{2\pi}{\hbar}\right)^2 |\bar{\epsilon}_1|^4 |\langle E_1,\hat{\mathbf{k}},q^- \,|\, D \,|\, E_i\rangle|^2 \tag{82}$$

$$P_q^{(12)}(E,\hat{\mathbf{k}}) = -2\left(\frac{2\pi}{\hbar}\right)^2 |\bar{\epsilon}_2 \bar{\epsilon}_1^2| \cos[\phi_2 - 3\phi_1 + \delta_q^{(12)}(\hat{\mathbf{k}})] |F_q^{(12)}(\hat{\mathbf{k}})| \tag{83}$$

Here, all channel indices $\mathbf{m}$ (which can be readily included) other than the final direction $\hat{\mathbf{k}}$ have been suppressed for clarity. The interference-amplitude $|F_q^{(12)}(\hat{\mathbf{k}})|$ and molecular-phase $\delta_q^{(12)}(\hat{\mathbf{k}})$ are defined by

$$|F_q^{(12)}(\hat{\mathbf{k}})| \exp\left(i\delta_q^{(12)}(\hat{\mathbf{k}})\right) = \langle E_i \,|\, D \,|\, E,\hat{\mathbf{k}},q^-\rangle \langle E,\hat{\mathbf{k}},q^- \,|\, \mathrm{d}_{e,g} \,|\, E_i\rangle \tag{84}$$

where D is the two-photon transition operator, given in lowest-order perturbation theory as

$$D = \sum_{e'} \mathrm{d}_{e,e'} (E_i - H_{e'} + \hbar\omega_1)^{-1} \mathrm{d}_{e',g} \tag{85}$$

The interference term $P_q^{(12)}(E,\hat{\mathbf{k}})$ is generally nonzero, so control over the differential cross section is possible.

Consider, however, the integral cross section into channel q,

$$P_q(E) = \int d\hat{\mathbf{k}}\, P_q(E,\hat{\mathbf{k}}) \tag{86}$$

and focus explicitly on the contribution from $P_q^{(12)}(E,\hat{\mathbf{k}})$. That is, consider

$$\begin{aligned} P_q^{(12)}(E) &= \int d\hat{\mathbf{k}} |F_q^{(12)}(\hat{\mathbf{k}})| \exp\left(i\delta_q^{(12)}(\hat{\mathbf{k}})\right) \\ &= \int d\hat{\mathbf{k}} \langle E_i, J_i, M_i \,|\, D \,|\, E,\hat{\mathbf{k}},q^-\rangle \langle E,\hat{\mathbf{k}},q^- \,|\, \mathrm{d}_{e,g} \,|\, E_i, J_i, M_i\rangle \end{aligned} \tag{87}$$

where we have explicitly inserted the angular momentum characteristics of the initial state, which is of energy E_i, angular momentum J_i, and projection M_i. Using the definition of D [Eq. (85)] and inserting unity in terms of the

states $|E_j, J_j, M_j\rangle$ of the intermediate electronic state we get,

$$P_q^{(12)}(E) = \sum_j \int d\hat{\mathbf{k}}[\hbar\omega_1 + E_i - E_j]^{-1} \langle E_i, J_i, M_i | \mathrm{d}_{g,e'} | E_j, J_j, M_j \rangle \times \langle E_j, J_j, M_j | \mathrm{d}_{e',e} | E, \hat{\mathbf{k}}, q^- \rangle \langle E, \hat{\mathbf{k}}, q^- | \mathrm{d}_{e,g} | E_i, J_i, M_i \rangle \quad (88)$$

The above expression must be zero because it embodies two contradictory requirements: Dipole selection rules as applied to $\langle E_i, J_i, M_i | \mathrm{d}_{g,e'} | E_j, J_j, M_j \rangle$ require that $J_j - J_i = \pm 1$, whereas by the same rules, $\langle E_j, J_j, M_j | \mathrm{d}_{e',e} | E, \hat{\mathbf{k}}, q^- \rangle \times \langle E, \hat{\mathbf{k}}, q^- | \mathrm{d}_{e,g} | E_i, J_i, M_i \rangle$ is nonzero only if $J_j - J_i = \pm 2, 0$. Hence $P_q^{(12)}(E)$ is zero; that is, coherent control over integral cross sections is not possible using the one-photon versus two-photon scenario. However, as noted above, control over the differential cross section is possible. A similar conclusion obtains for any N-photon versus M-photon process where N and M are of different parities.

Experimental implementations of the one-plus-two photon absorption scenario have taken a variety of forms (Baranova *et al.*, 1990; Yin *et al.*, 1992, 1995; Dupont, 1995; Sheeny *et al.*, 1995). For example, Corkum and coworkers (Dupont *et al.*, 1995) have carried out one-photon versus two-photon absorption in crafted quantum wells to demonstrate control over the directional motion of the excited electron. Sipe, van Driel, and coworkers (Hache *et al.*, 1997) have extended this work to the complex case of bulk semiconductors. Following the theoretical work of Charron *et al.* (1995), Sheeny *et al.* (1995) have used this scenario to control product directionality in HD^+ dissociation to $H + D^+$ and $H^+ + D$.

3. *Two-Photon versus Two-Photon Interference*

Here we show that by considering (resonantly enhanced) two-photon versus two-photon dissociation, it is possible to maintain control in a molecular system in thermal equilibrium. The resonant character of the excitations is important because in this way only one state, out of the ensemble of thermally populated molecular states, participates in the photo-dissociation. As shown below, it is also possible in this way to overcome phase jitter in the laser sources.

Consider first photo-dissociation due to the absorption of two photons, of frequency ω_1 and ω_2, where the first photon is assumed resonant with an intermediate bound level. In this process a molecule, initially in a state $|E_i, J_i, M_i\rangle$, is photo-dissociated because of a combination of two CW fields,

$$\epsilon(t) = 2\mathcal{R}_e[\hat{\epsilon}_2 \bar{\epsilon}_2 \exp(-i\omega_2 t) + \hat{\epsilon}_1 \bar{\epsilon}_1 \exp(-i\omega_1 t)] \quad (89)$$

to yield a number of different product channels labeled by q. The near-resonance condition means that absorption of the first photon, of frequency

ω_1, lifts the system to a region close to an intermediate bound state $|E_m J_m M_m\rangle$. The second photon, of frequency ω_2, further excites the system to a dissociating state $|E, \mathbf{k}, q^-\rangle$. The probability-amplitude $D_{\mathbf{k}q}(E, E_i J_i M_i, \omega_2, \omega_1)$ for resonant two-photon $(\omega_1 + \omega_2)$ dissociation is given by (Chen *et al.*, 1993b)

$$D_{\mathbf{k}q}(E, E_i J_i M_i, \omega_2, \omega_1) = \bar{\epsilon}_2 \bar{\epsilon}_1 \sum_{e' E_m, J_m} \frac{\langle E, \mathbf{k}q^- | \mathrm{d}_{e,e'} | E_m J_m M_i \rangle \langle E_m J_m M_i | d_{e',g} | E_i J_i M_i \rangle}{E_i + \hbar\omega_1 - E_m - \Delta_m + i\Gamma_m/2} \tag{90}$$

Here $E = E_i + (\omega_1 + \omega_2)\hbar$, and Δ_m and Γ_m are respectively the radiative shift and width of the intermediate state.

As a consequence of the form of the denominator in Eq. (90), the photo-dissociation probability, given by the square of $D_{\mathbf{k}q}$, is greatly enhanced by the inverse square of the detuning $\Delta = E_i + \hbar\omega_1 - E_m - \Delta_m + i\Gamma_m/2$. Hence, only the levels closest to the resonance $\Delta = 0$ contribute significantly to the dissociation probability. Ideally, this allows us selectively to photo-dissociate a single state from a thermal bath. This holds true as long as the line width Γ_m is less than Δ and the spacings between neighboring transitions are smaller than the laser bandwidth.

Consider now the simultaneous excitation by *two* resonant two-photon routes using three interrelated frequencies, $\omega_0, \omega_+, \omega_-$ with associated field amplitudes and phases denoted as $\bar{\epsilon}_0, \bar{\epsilon}_+, \bar{\epsilon}_-$, and $\theta_0, \theta_+, \theta_-$, respectively, where ω_0 and ω_+ are chosen resonant with intermediate bound-state levels. Choosing the three frequencies such that $2\omega_0 = \omega_+ + \omega_-$, we can make the absorption of $2\omega_0$ photons (pathway "*a*") interfere with the absorption of an ω_+ and an ω_- photon (pathway "*b*"), because $E_i + 2\omega_0 = E_i + (\omega_+ + \omega_-) = E$. The probability of photo-dissociation at energy E into arrangement channel q is therefore given as the square of the sum of the two-photon amplitude of pathway "*a*" and the two-photon amplitude of pathway "*b*":

$$\begin{aligned} P_q(E, E_i J_i M_i; \omega_0, \omega_+, \omega_-) &\equiv \int d\mathbf{k} |D_{\mathbf{k}q}(E, E_i J_i M_i, \omega_0, \omega_0) + D_{\mathbf{k}q}(E, E_i J_i M_i, \omega_+, \omega_-)|^2 \\ &\equiv P_q(a) + P_q(b) + P_q(ab) \end{aligned} \tag{91}$$

Here $P_q(a)$ and $P_q(b)$ are the independent photo-dissociation probabilities associated with routes a and b respectively and $P_q(ab)$ is the interference term between them,

$$P_q(ab) = 2|F_q(ab)| \cos(\delta_q^a - \delta_q^b + 2\theta_0 - \theta_+ - \theta_-) \tag{92}$$

where the interference-amplitude $|F_q(ab)|$ and the molecular phase difference $(\delta_q^a - \delta_q^b)$ are defined via the equation

$$|F_q(ab)| \exp[i(\delta_q^a - \delta_q^b)] = D_{\mathbf{k}q}(E, E_i J_i M_i, \omega_0, \omega_0) D_{\mathbf{k}q}^*(E, E_i J_i M_i, \omega_+, \omega_-) \tag{93}$$

We see that control over the the quantity of interest, the channel branching ratio $R_{qq'}$, can be attained, as in previous scenarios, by varying such quantities as the $(2\theta_0 - \theta_+ - \theta_-)$ phase difference and the $(x = |\bar{\epsilon}_+ \bar{\epsilon}_- / \bar{\epsilon}_0^2|)$ amplitude ratio. Besides the ability to work in a thermal environment, the great advantage of this control scenario is that the $(2\theta_0 - \theta_+ - \theta_-)$ relative phase term allows for the cancellation of individual phase jitters arising in each laser source. For example, one can generate the ω_+ and ω_- frequencies by frequency summing $\omega_+ = \omega_0 + \delta$ and frequency differencing $\omega_- = \omega_0 - \delta$ with a third source of frequency δ. Because ω_+ and ω_- are generated in this way, the phase difference $2\theta_0 - \theta_+ - \theta_-$ between path (a) and path (b) vanishes (Schubert and Wilhelmi, 1986). Thus, fluctuations in θ_0 or δ cancel and have no effect on the interference term.

To demonstrate the range of control afforded by this scheme, consider the photo-dissociation of the Na_2 molecule in $v_i = J_i = 0$ [Fig. 4] to form the Na(3*s*) + Na(3*p*) and Na(3*s*) + Na(4*s*) products. As the $|E_m J_m M_m\rangle$ intermediate resonance we choose vib-rotational states belonging to the spin-orbit coupled $A^1\Sigma_u^+$ and $b^3\Pi_u$ electronic manifolds (Chen *et al.*, 1993b). Despite the multitude of electronic states involved in the process, the predominant contributions to the products Na(3*s*) + Na(3*p*) and Na(3*s*) + Na(4*s*) are found to come (Chen *et al.*, 1993b) from the $^3\Pi_g$ and $^3\Sigma_g^+$ states.

Typical control results are shown in Fig. 5, which shows a contour plot of the Na(3*s*) + Na(4*s*) yield as a function of the ratio of the laser amplitudes x, and of the relative laser phase $\delta\theta = 2\theta_0 - \theta_+ - \theta_-$. We show the results of photo-dissociation with wavelengths $\lambda_0 = 594.505$ nm, $\lambda_+ = 582.057$ nm, and $\lambda_- = 607.498$ nm (corresponding to ω_0, ω_+, and ω_-) excited via the $^1\Sigma_u^+$ $v_m = 13$ and 18, $J_m = 1$ intermediate states. The range of control is considerable, with the Na(4*s*) yield varying from 10% to 51% as $\delta\theta$ is varied.

Experimental demonstrations of this scenario for the ionization of atomic Ba (Wang *et al.*, 1996b) and NO (Pratt, 1996) have been reported.

4. *Polarization Control of Differential Cross Sections*

Rather than attempting coherent control with two different frequencies, it would seem that the use of two different polarizations of the same frequency would be much easier to implement experimentally. It turns out that this

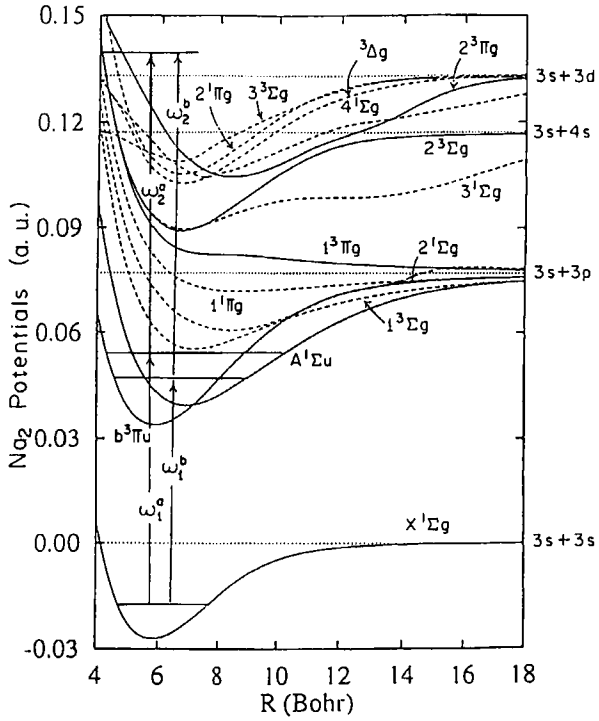

FIG. 4. Na_2 potential energy surfaces relevant to the two-photon versus two-photon control scenario. The arrows indicate the resonant two-photon versus two-photon pathways included in the computation discussed here. (From Chen *et al.*, 1993a.)

scenario is akin to the one-photon versus two-photon control in the sense that integral control is not possible. Further, though differential cross sections can be controlled (Asaro *et al.*, 1988), there is no breaking of the forward-backward symmetry in this case.

In order to see this, we consider the photo-dissociation of a *single* bound state $|E_1\rangle$ by a single CW source of the type

$$\epsilon = \epsilon_1 \exp(i\alpha_1)\hat{\epsilon}_1 + \epsilon_2 \exp(i\alpha_2)\hat{\epsilon}_2$$

where $\hat{\epsilon}_1$ and $\hat{\epsilon}_2$ are two orthonormal vectors.

We can regard the two components $\hat{\epsilon}_1$ and $\hat{\epsilon}_2$ as inducing two independent excitation routes. Choosing $\hat{\epsilon}_1$ and $\hat{\epsilon}_2$ parallel and perpendicular to the quantization (z) axis, respectively, the differential cross section is composed of three terms; one corresponds to photo-dissociation of $|E_1\rangle$ by the $\hat{\epsilon}_1$ component, one corresponds to photo-dissociation of $|E_1\rangle$ by the $\hat{\epsilon}_2$ component, and one is the cross term between these two contributions. Excitation by the parallel

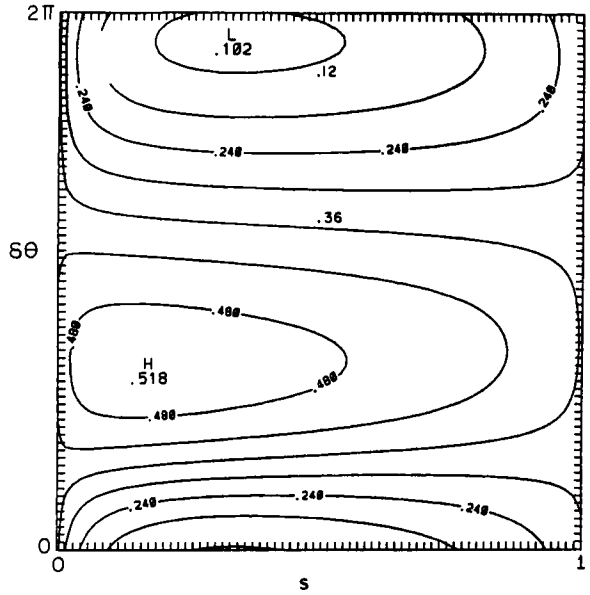

FIG. 5. Contours of equal Na(4s) yield in the controlled photo-dissociation of Na_2, initially in vibrational state $v = 10$. The ordinate is the relative laser phase, and the abscissa is the field intensity ratio s. (From Chen *et al.*, 1993a.)

component allows $\Delta M_J = 0$ transitions, whereas excitation by the perpendicular $\hat{\epsilon}_2$ component allows $\Delta M_J = \pm 1$ transitions. The interference term is therefore comprised of a product of two bound-continuum matrix elements, where the two continua differ in M_J by ± 1. If this cross term is nonzero, then control over the differential cross section is possible. However, producing the integral cross section necessitates integrating the differential cross section over $\hat{\mathbf{k}}$, and under these circumstances, the cross term vanishes. Contrary to the one-photon versus two-photon case, the states comprising the $|E, \hat{\mathbf{k}}^-\rangle$ state are of the same parity. Thus the backward-forward symmetry is not broken. The control manifests itself in our ability to sharpen or broaden the angular distribution about a given recoil direction.

Polarization control in intense fields has been proposed as a means of generating subfemtosecond pulses (Ivanov *et al.*, 1995), but it has yet to be demonstrated experimentally.

B. PUMP-DUMP CONTROL: TWO-LEVEL EXCITATION

Control of the dynamics via a pump-dump scenario was first introduced by Tannor and Rice (1985). These authors emphasized the localized wavepacket aspects of pump-dump control, entailing the excitation of, and interference

between, many levels. In this section, we consider excitation of only two levels. It can be regarded as the pulsed analog of the bichromatic control with a superposition state outlined in Section III.

Consider a molecule, initially ($t = 0$) in an eigenstate $|E_1\rangle$ of the molecular Hamiltonian H_M, which is subjected to two transform-limited light pulses. The electric field $\epsilon(t)$ consists of two temporally separated pulses

$$\epsilon(t) = \epsilon_x(t) + \epsilon_d(t) \tag{94}$$

The pump pulse $\epsilon_x(t)$ induces a transition to a linear combination of the eigenstates $|E_i\rangle$ of the excited electronic state. Though the pump pulse may be chosen to encompass any number of states, here we choose it sufficiently narrow to excite only a superposition of two states $|E_2\rangle$ and $|E_3\rangle$. The dump pulse $\epsilon_d(t)$ dissociates the molecule by further exciting this superposition state to the continuous part of the spectrum. Both fields are chosen sufficiently weak for perturbation theory to be valid.

For convenience we use Gaussian pulses that peak at $t = t_x$ and t_d, respectively. In particular, the excitation pulse is of the form

$$\varepsilon_x(t) = (\epsilon_x/\tau_x)\exp[-i(\omega_x t + \delta_x)]\exp[-(t - t_x)^2/\tau_x^2] \tag{95}$$

The associated frequency profile is given by

$$\bar{\epsilon}_x(\omega) = (\sqrt{\pi}/2)\epsilon_x\tau_x\exp[-i(\omega_x - \omega)t_x]\exp[-\tau_x^2(\omega_x - \omega)^2/4]\exp(-i\delta_x) \tag{96}$$

By writing $\bar{\epsilon}_x(\omega) = |\bar{\epsilon}_x(\omega)|e^{i\phi(\omega)}$, we see that $\phi(\omega) = (\omega - \omega_x)t_x - \delta_x$. The analogous quantities $\epsilon_d(t)$ and $\bar{\epsilon}_d(\omega)$ are defined similarly, with the parameters t_d and ω_d replacing t_x and ω_x, etc.

Because the two pulses are temporally distinct, it is convenient to deal with each of their effects independently. The superposition state prepared after the $\epsilon_x(t)$ pulse is over is given in first-order perturbation theory as

$$|\phi(t)\rangle = |E_1\rangle e^{-iE_1t/\hbar} + b_2|E_2\rangle e^{-iE_2t/\hbar} + b_3|E_3\rangle e^{-iE_3t/\hbar} \tag{97}$$

where [Eq. (8)]

$$b_k = (2\pi i/\hbar)\langle E_k|\mathbf{d}\cdot\hat{\epsilon}|E_1\rangle\bar{\epsilon}_x(\omega_{k,1}),\ k = 2,3 \tag{98}$$

with $\omega_{k,1} \equiv (E_k - E_1)/\hbar$.

After a delay time of $\tau \equiv t_d - t_x$, the system is subjected to the $\epsilon_d(t)$ pulse. It follows from Eq. (97) that at that time, each preparation coefficient has

picked up an extra phase factor of $e^{-iE_k\tau/\hbar}, k = 2, 3$. Hence, the phase of b_2 relative to b_3 at that time increases by $[-(E_2 - E_3)\tau/\hbar = \omega_{3,2}\tau]$. Thus the natural two-state time evolution controls the relative phase of the two terms, replacing the externally controlled relative laser phase of the bichromatic control scenario of Section III.

After the conclusion of the $\epsilon_d(t)$ pulse, the system wavefunction is given as

$$|\psi(t)\rangle = |\phi(t)\rangle + \sum_{q,\mathbf{m}} \int dE\, b_{E,q,\mathbf{m}}(t) |E, q, \mathbf{m}^-\rangle e^{-iEt/\hbar} \tag{99}$$

The probability of observing the q product at total energy E in the remote future is therefore given by

$$\begin{aligned} P_q(E) &= \sum_{\mathbf{m}} |b_{E,q,\mathbf{m}}(t = \infty)|^2 \\ &= (2\pi/\hbar^2) \sum_{\mathbf{m}} \left| \sum_{k=2,3} b_k \exp(-iE_k\tau/\hbar) \langle E, q, \mathbf{m}^- | \mathbf{d}_{e,e'} | E_k \rangle \bar{\epsilon}_d(\omega_{EE_k}) \right|^2 \end{aligned} \tag{100}$$

where $\omega_{EE_k} = (E - E_k)/\hbar$, b_k is given by Eq. (98), and $\bar{\epsilon}_d(\omega_{EE_k})$ is given via an expression analogous to Eq. (96).

Expanding the square gives

$$\begin{aligned} P_q(E) = \left(\frac{2\pi}{\hbar^2}\right) &[|b_2|^2 \mu_q(22) \bar{\epsilon}_2^2 + |b_3|^2 \mu_q(33) \bar{\epsilon}_3^2 \\ &+ 2|b_2 b_3^* \bar{\epsilon}_2 \bar{\epsilon}_3^* \mu_q(23)| \cos(\omega_{32}\tau + \alpha_q(23) + \chi)] \end{aligned} \tag{101}$$

where $\bar{\epsilon}_i = |\bar{\epsilon}_d(\omega_{EE_i})| e^{i\phi(\omega_{EE_i})}$, $\omega_{32} = (E_3 - E_2)/\hbar$, and the phases χ, $\alpha_q(23)$ are defined via

$$\begin{aligned} \langle E_1 | \mathbf{d}_{e',g} | E_g \rangle \langle E_g | \mathbf{d}_{g,e'} | E_2 \rangle &\equiv |\langle E_1 | \mathbf{d}_{e',g} | E_g \rangle \langle E_g | \mathbf{d}_{g,e'} | E_2 \rangle| e^{i\chi} \\ \mu_q(ik) \equiv |\mu_q(ik)| e^{i\alpha_q(ik)} &= \sum_{\mathbf{m}} \langle E, q, \mathbf{m}^- | \mathbf{d}_{e,e'} | E_i \rangle \langle E_k | \mathbf{d}_{e',e} | E, q, \mathbf{m}^- \rangle \end{aligned} \tag{102}$$

Integrating Eq. (101) over E to encompass the full width of the second pulse yields the final expressions for the quantities we wish to control: P_q, the probability of forming channel q, and $R_{q,q'}$, the ratio of product probabilities into q versus q'.

Examination of Eq. (101) makes clear that $R_{q,q'}$ can be varied by changing the delay time $\tau = (t_d - t_x)$ or the ratio $x = |b_2/b_3|$; the latter is most conveniently done by detuning the initial excitation pulse. Note that once again, as in the scenarios above, the z dependence of P_q vanishes because of cancellation between the excitation and dump steps. In addition, the phases δ_x, δ_d do not appear in the final result, so the relative phases of the two pulses do not affect the result.

To gain insight into the control afforded by this scenario, we initially applied (Seideman *et al.*, 1989) it to a model collinear branching photo-dissociation reaction with masses of D and H, i.e.,

$$H + HD \leftarrow DH_2 \rightarrow D + H_2 \tag{103}$$

in which one uses the first pulse to excite a pair of states in an electronic state supporting bound states and the second pulse to dissociate the system by de-exciting it back to the ground state, above the dissociation threshold.

Typical control results (Seideman *et al.*, 1989) are displayed in Fig. 6, which shows contours of equal DH yield as a function of $E_x - E_{AV}$ and τ. Here $(E_x - E_{AV})$ measures the deviation of the central excitation energy of the pump pulse from the average energy E_{AV} of the pair of bound states it excites. The DH yield is shown to vary significantly, from 16% to 72%, as the control parameters are varied. This is an extreme range of control, especially if one considers that the product channels differ by only a mass factor.

It is highly instructive to examine the nature of the superposition state prepared in the initial excitation, [Eq. (97)] and its time evolution during the delay between pulses. An example is shown in Fig. 7, where we plot the wavefunction for a collinear model of DH_2 photo-dissociation [Eq. (103)]. Specifically, the axes are the H + HD reaction coordinate S and its orthogonal conjugate x. The wavefunction is shown evolving over half of its total possible period. An examination of Fig. 6 in conjunction with Fig. 7 shows that de-exciting this superposition state at the time of panel (b) would result in a substantially different product yield than de-exciting at the time of panel (e). However, Fig. 7 shows that there is clearly no particular preference of the wavefunction for either large positive or large negative S at these particular times, which would be the case if the reaction control were a result of some spatial characteristics of the wavefunction. Rather, the results make clear that the essential control characteristics of the wavefunction are encrypted in the quantum amplitude and phase of the created superposition state.

The pump-dump scheme has also been applied (Abrashkevich *et al.*, 1998b) (computationally) to the photo-dissociation of a fully realistic representation of Li_2 to control the cross sections for production of Li(2s) + Li(2p), Li(2s) + Li(3p) and Li(2s) + Li(3s). In particular, a CW laser was

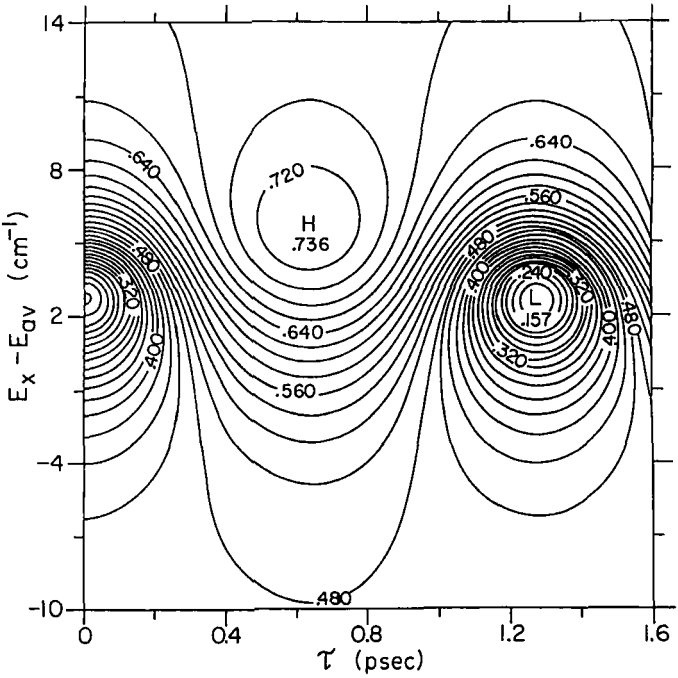

FIG. 6. Contour plot of the DH yield as a function of the detuning of the exciting pulse $E_x - E_{av}$ and the delay variable τ. In this case the time between pulse centers is $\Delta T = (8.44 + 2.11n)ps + \tau$, ensuring nonoverlapping pulses and allowing for arbitrary positive integer n. Here the initially created superposition state is between levels 56 and 57 ($E_1 = 0.323\,849$ a.u., $E_2 = 0.323\,968$ a.u.) of the G1 surface. The letters H and L denote the positions of the absolute maxima and minima, whose magnitudes are explicitly shown. (From Seideman *et al.*, 1989.)

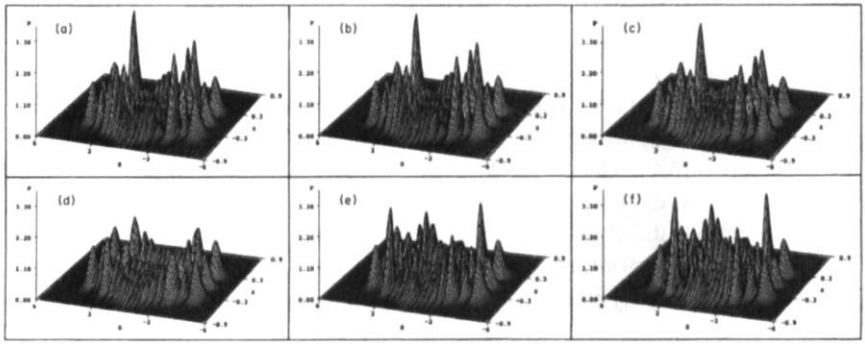

FIG. 7. Time evolution of the square of the wavefunction for a superposition state comprised of levels 56 and 57. The probability is shown as a function of S and its orthogonal coordinate x at times (a) 0, (b) 0.0825 ps, (c) 0.165 ps, (d) 0.33 ps, (e) 0.495 ps, and (f) 0.66 ps, which correspond to equal fractions of one half of the period $2\pi/\omega_{2,1}$. (From Seideman *et al.*, 1989.)

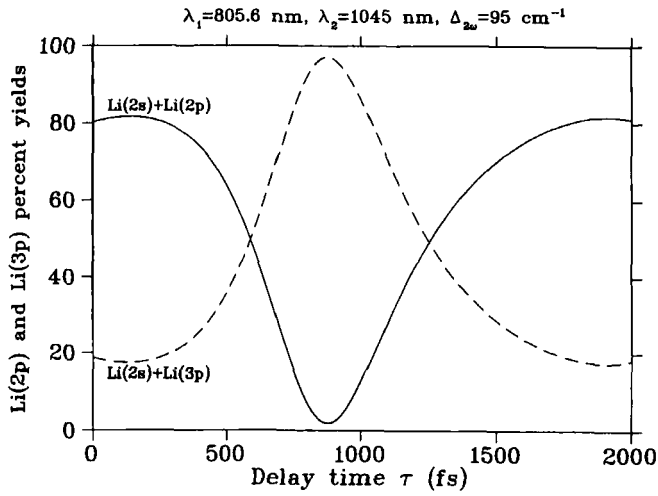

FIG. 8. Li(2p) and Li(3p) yields in the pump-dump controlled photo-dissociation of Li_2 as a function of the delay between pulses. Wavelengths of the two pulses, as well as the frequency width of the second pulse, are indicated. (From Abrashkevich *et al.*, 1998b.)

used to prepare a single rovibrational state of the $A^1\Sigma_u^+$ electronically excited state. Subsequent pump-dump excitation allowed extensive control over product yields with, for instance, Li(2s) + Li(2p) ranging from 2% to 82% as the time delay between pulses is varied over 1 ps. Simultaneously, as seen in Fig. 8, the Li(2s) + Li(3p) product is exactly out of phase so that we have almost total control over the Li(3p) to Li(2p) ratio. Computations have also been done on the control of the polyatomic system:

$$D + OH \leftarrow HOD \rightarrow H + OD$$

via the B-state of HOD (Shapiro and Brumer, 1993).

Note, finally, that control is sensitive to the degree of laser coherence. If the pump laser is only partially coherent (Jiang and Brumer, 1991), then control can be significantly degraded (Jiang *et al.*, 1996). This is not the case for the dump pulse, where a significant degree of laser incoherence can be tolerated.

Experimental studies of pump-dump control fall into two categories: (a) the large number of pump-dump experiments where the dump pulse is used as a probe of the previously prepared dynamics (Potter *et al.*, 1992; Baumert *et al.*, 1991) but that can be interpreted as demonstrations of pump-dump control; and (b) those expressly designed to demonstrate coherent control. The latter category includes work by Wilson (Bardeen *et al.*, 1997), Silberberg (Yelin *et al.*, 1997), and Gerber (Assion *et al.*, 1998). For example, Gerber *et al.* controlled the ratio of $CpFeCOCl^+/FeCl^+$ products in the photo-fragmentation

of $CpFe(CO)_2Cl$ using pulsed and chirped femtosecond sources, opening the way for laser control of large molecular systems.

C. Symmetry Breaking and the Generation of Chirality

Symmetry breaking occurs in nature whenever a system undergoes a (spontaneous or forced) transition to a *nonsymmetric* eigenstate (i.e., states that do not belong to any of the representations of the symmetry group) of the Hamiltonian. Such nonsymmetric eigenstates occur if there exist several degenerate eigenstates, each belonging to a different irreducible symmetry representation, because a linear combination of eigenstates of different symmetry will in general be nonsymmetric.

Nonsymmetric eigenstates of a symmetric Hamiltonian occur naturally in the continuous spectrum of a *BAB* type molecule. It is clear that the $|E, \mathbf{m}, R^-\rangle$ state, which correlates asymptotically with the dissociation of the right *B* group, must be degenerate with the $|E, \mathbf{m}, L^-\rangle$ state, which correlates with the departure of the *B* group on the left-hand side. Hence, any experiment performed in the asymptotic $B + AB$ or $BA + B$ regions must, by necessity, measure the probability of populating a nonsymmetric state. It is also possible to form *symmetric* $|E, \mathbf{m}, s^-\rangle$ and *antisymmetric* $|E, \mathbf{m}, a^-\rangle$ eigenstates of the same Hamiltonian by taking the plus and minus combinations of nonsymmetric states. However, symmetric and antisymmetric states are not directly observable in the asymptotic regime.

We may say that the very act of observation of the dissociated molecule entails the collapse of the system to one of the nonsymmetric states. Because the probability of collapse to the $|E, \mathbf{m}, R^-\rangle$ state is equal to the probability of collapse to the $|E, \mathbf{m}, L^-\rangle$ state, the collapse to a nonsymmetric state does not lead to a preference of *R* over *L* in an *ensemble* of molecules. The above collapse is due to (random) factors that are not in our control. Coherent control techniques do not change this "*spontaneous symmetry breaking*" aspect of quantum mechanics. Rather, as we show below, it allows us to bias the *a priori* probability of producing the *R* or the *L* form.

One of the most important cases of symmetry breaking arises when the two *B* groups (now denoted as *B* and *B'*) are not identical but are enantiomers of each other. (Two molecules are said to be enantiomers of each other if one is the mirror image of the other. If these groups are also "chiral", i.e., if they lack a center of inversion symmetry, then the two enantiomers are distinguishable and can be detected through the distinctive direction of rotation of linearly polarized light).

The existence and role of enantiomers are recognized as one of the fundamental broken symmetries in nature (Barron, 1982; Woolley, 1975; Walker, 1979). It has motivated a long-standing interest in asymmetric synthesis, i.e.,

processes that preferentially produce specific chiral species. Contrary to the prevailing belief (Barron, 1986) that asymmetric synthesis must involve either chiral reactants or chiral external system conditions such as chiral crystalline surfaces, we have shown (Shapiro and Brumer, 1991) (and review below) that preferential production of a chiral photofragment can occur even though the parent molecule is not chiral. In particular, two results have been demonstrated (Shapiro and Brumer, 1991): (1) ordinary photo-dissociation, using linearly polarized light, of a BAB' "pro-chiral" molecule can yield different cross sections for the production of right-handed (B) and left-handed (B') products if the projection of the angular momentum (m_j) of the products is selected; and (2) this natural symmetry breaking may be enhanced and controlled using coherent control.

To treat this problem, consider the pump-dump scenario described in Section V.B, with attention focused on control of the relative yield of two product arrangement channels, where the product angular momentum projection m_j is fixed. That is, we consider $P_q(E; m_j)$ with q labeling either the right- ($q = R$) or the left- ($q = L$) handed product.

As above, the product ratio $R_{qq'} = P_R(E; m_j)/P_L(E; m_j)$ is a function of the delay time $\tau = (t_d - t_x)$ and the ratio $x = |c_1/c_2|$, the latter by varying the energy of the initial excitation pulse. Active control over the products $B + AB'$ versus $B' + AB$, i.e., a variation of $R_{qq'}$ with τ and x, and hence control over left- versus right-handed products, will result only if $P_R(E; m_j)$ and $P_L(E; m_j)$ have different functional dependences on the control parameters x and τ.

To show that $P_R(E; m_j)$ may differ from $P_L(E; m_j)$ for the $B'AB$ case, note first that this molecule belongs to the C_s point group. This group possesses only one plane of symmetry, denoted σ, which is defined as the collection of points satisfying the requirement that the $B - A$ distance equals the $A - B'$ distance. Furthermore, we shall focus upon transitions between electronic states of the same representations, e.g., A' to A' or A'' to A'' (where A' denotes the symmetric representation and A'' the antisymmetric representation of the C_s group). We further assume that the ground vibronic state belongs to the A' representation.

To obtain control, we wish to choose the intermediate state $|E_3\rangle$ to be *symmetric* and the intermediate state $|E_2\rangle$ to be *antisymmetric* with respect to reflection in the σ-plane. Hence we first demonstrate that it is possible optically to excite, simultaneously, both the symmetric $|E_3\rangle$ and the antisymmetric $|E_2\rangle$ states. Using Eq. (98) we see that this requires the existence of both a dipole component that is symmetric, denoted $d^s_{e',g}$, and a component that is antisymmetric, denoted $d^a_{e',g}$, because by the symmetry properties of $|E_3\rangle$ and $|E_2\rangle$,

$$\langle E_3 | d_{e',g} | E_1 \rangle = \langle E_3 | d^s_{e',g} | E_1 \rangle, \langle E_2 | d_{e',g} | E_1 \rangle = \langle E_2 | d^a_{e',g} | E_1 \rangle \quad (104)$$

Both dipole-moment components do occur in $A' \rightarrow A'$ electronic transitions whenever a bent $B' - -A - -B$ molecule deviates considerably from the equal-distance C_{2v} geometries (where $d^a = 0$). The effect is non–Franck-Condon in nature because the dipole moment must vary with the nuclear configurations. In the terminology of the theory of vibronic transitions, both symmetric and antisymmetric components can be nonzero because of a Herzberg-Teller intensity borrowing (Hollas, 1982) mechanism. It is therefore the case that the excitation pulse can create a $|E_3\rangle, |E_2\rangle$ superposition consisting of two states of different reflection symmetry, a state that is therefore nonsymmetric.

We now show that the nonsymmetry created by this excitation of *nondegenerate* bound states translates to a nonsymmetry in the probability of populating the *degenerate* $|E, \mathbf{m}, R^-\rangle$, $|E, \mathbf{m}, L^-\rangle$ continuum states. To do so we examine the properties of the bound-free transition matrix elements $\langle E, q, \mathbf{m}^-|\mathrm{d}_{e,e'}|E_k\rangle$ that enter into the probability of dissociation [Eq. (100)]. Note first that although the continuum states $|E, q, \mathbf{m}^-\rangle$ are nonsymmetric, we can define symmetric and antisymmetric continuum eigenfunctions $|E, \mathbf{m}, s^-\rangle$ and $|E, \mathbf{m}, a^-\rangle$ via the relations

$$|E, \mathbf{m}, R^-\rangle \equiv [|E, \mathbf{m}, s^-\rangle + |E, \mathbf{m}, a^-\rangle]/\sqrt{2} \tag{105}$$

$$|E, \mathbf{m}, L^-\rangle \equiv [|E, \mathbf{m}, s^-\rangle - |E, \mathbf{m}, a^-\rangle]/\sqrt{2} \tag{106}$$

Note that $\sigma|E, \mathbf{m}, R^-\rangle = |E, \mathbf{m}, L^-\rangle$. Using the fact that $|E_3\rangle$ is symmetric and $|E_2\rangle$ is antisymmetric, and adopting the notation $a_{s2} \equiv \langle E, \mathbf{m}, \mathbf{s}^-|d^a_{e',g}|E_2\rangle$, $s_{a3} \equiv \langle E, \mathbf{m}, a^-|\mathrm{d}^s_{e,e'}|E_3\rangle$, etc., we have [see Eq. (102)],

$$\mu_q(33) = \sum_{\mathbf{m}} [|s_{s3}|^2 + |a_{a3}|^2 \pm 2\mathcal{R}_e(a_{a3}\, s^*_{s3})] \tag{107}$$

$$\mu_q(22) = \sum_{\mathbf{m}} [|a_{s2}|^2 + |s_{a2}|^2 \pm 2\mathcal{R}_e(a_{s2}\, s^*_{a2})] \tag{108}$$

$$\mu_q(32) = \sum_{\mathbf{m}} [s_{s3}\, a^*_{s2} + a_{a3}\, s^*_{a2} \pm s_{s3}\, s^*_{a2} \pm a_{a3}\, a^*_{s2}] \tag{109}$$

where the plus sign applies for $q = R$, the minus sign applies for $q = L$, and $\mu_q(23) = \mu^*_q(32)$. Equation (109) displays two noteworthy features:

1. $\mu_L(kk) \neq \mu_R(kk), k = 2, 3$. That is, the system displays *natural symmetry breaking* in photo-dissociation from state $|E_3\rangle$ or state $|E_2\rangle$, with right- and left-handed product probabilities differing by

$4\Sigma_{\mathbf{m}}\,\mathcal{R}_e(s^*_{s3}a_{a3})$ for excitation from $|E_3\rangle$ and by $4\Sigma_{\mathbf{m}}\,\mathcal{R}_e(a_{s2}s^*_{a2})$ for excitation from $|E_2\rangle$. Note that these symmetry-breaking terms exist only if the transition dipole operator possesses both a symmetric and an antisymmetric component, which can occur only if the Franck-Condon approximation breaks down.

2. $\mu_L(23) \neq \mu_R(23)$. If the Franck-Condon approximation holds, there is no "natural" symmetry breaking of the type discussed above. However, even when the FC approximation holds, $\mu_L(23) \neq \mu_R(23)$ and laser-controlled symmetry breaking according to Eq. (101) is possible.

To demonstrate the range of expected control, we consider a model of enantiomer selectivity (Shapiro and Brumer, 1991), i.e., HOH photo-dissociation in three dimensions, where the two hydrogens are assumed distinguishable:

$$\mathrm{HO} + \mathrm{H} \leftarrow \mathrm{HOH} \rightarrow \mathrm{H} + \mathrm{OH}$$

The computation of $R_{qq'}$, the HO + H (as distinct from the H + OH) product for polarized OH fragments, was done using the formulation and computational methodology of Segev and Shapiro (1982) and Balint-Kurti and Shapiro (1981). Figure 9 shows the result of first exciting the superposition of symmetric plus antisymmetric vibrational modes $[(1, 0, 0) + (0, 0, 1)]$ with rotational quantum numbers $J_i = J_k = 0$ in the ground electronic state,

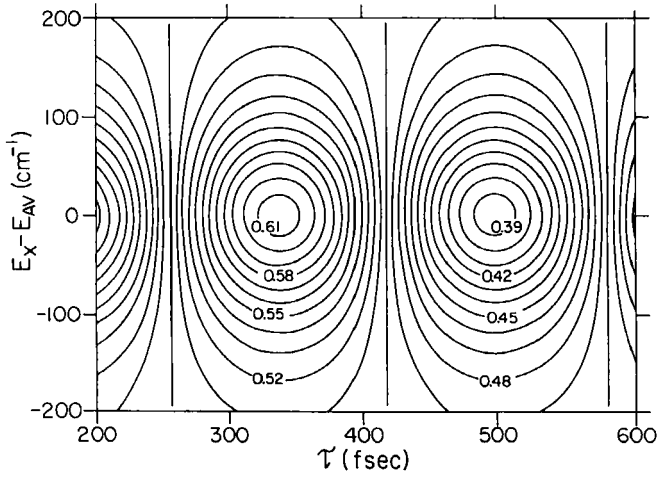

FIG. 9. Contour plot of percent HO + H (as distinct from H + OH) in HOH photodissociation. The ordinate is the detuning from $E_{av} = (E_2 - E_1)/2$, and the abscissa is the time delay between pulses. (From Shapiro and Brumer, 1991.)

followed by dissociation at 70,700 cm^{-1} to the B state using a pulse width of 200 cm^{-1}. Results show that varying the time delay between pulses allows for controlled variation of $R_{qq'}$ from 61% to 39%!

Finally, we discuss symmetry breaking and chirality control with *unpolarized* OH fragments where a summation over the magnetic quantum number m_j is performed. It can be shown that summing over m_j eliminates all contributions to Eq. (109) that involve both $|E, \mathbf{m}, a^-\rangle$ and $|E, \mathbf{m}, s^-\rangle$, and as a result,

$$\mu_L(kk) = \mu_R(kk) = \sum_i [|s_{si}|^2 + |a_{ai}|^2] \tag{110}$$

$$\mu_L(23) = \mu_R(23) = \sum_{i,j} [s_{si} a^*_{sj} + a_{ai} s^*_{aj}] \tag{111}$$

That is, natural symmetry breaking is lost upon m_j summation, both channels $q = R$ and $q = L$ having equal photo-dissociation probabilities, and control over the enantiomer ratio is lost because the interference terms, which still exist, no longer distinguish the $q = R$ and $q = L$ channels.

VI. Strong-Field Incoherent Interference Control

In this section we discuss both the theory and an experiment of an elegant strong-field laser control scenario. As we saw above, the quantum nature of weak-field CC manifests itself in the sensitivity of the outcome to a change in an external *phase*. In contrast, under some strong-field situations, the interference term may become independent of the phase of the light sources involved, which therefore no longer need be coherent. Instead of the phase, the interference term now becomes sensitive to the relative *frequency* between the two light sources. We call the resulting control scenario "incoherent interference control" (IIC) (Chen *et al.*, 1995). The above two features are very favorable from the experimental point of view because one can use conventional non-transform-limited lasers and molecules in thermal environments. Indeed, an experimental realization of IIC has already been reported (Shnitman *et al.*, 1996).

In general terms, the IIC scenario operates as follows: Consider a molecule in an initial bound state $|E_i\rangle$ that absorbs two photons of frequency ω_1 and, in doing so, is excited to a continuum state $|E, q, \mathbf{m}^-\rangle$ via a resonant intermediate state $|E_{j_1}\rangle$. The outcome of this photo-dissociation process can be controlled by applying a "control laser" ω_2 that couples initially unpopulated bound states $|E_{j_2}\rangle$ to the same continuum. With both lasers on, dissociation to $|E, q, \mathbf{m}^-\rangle$ occurs via numerous dissociation pathways. To lowest order,

these are the routes $|E_i\rangle \rightarrow |E_{j_1}\rangle \rightarrow |E, q, \mathbf{m}^-\rangle$ as well as $|E_i\rangle \rightarrow |E_{j_1}\rangle \rightarrow |E', q', \mathbf{m}'^-\rangle \rightarrow |E_{j_2}\rangle \rightarrow |E, q, \mathbf{m}^-\rangle$, etc. Contributions from these multiple pathways to the product in a given channel q at energy E interfere (either constructively or destructively) with one another. Varying the frequency and intensity of the control laser alters the interference and hence the dissociation line shape and the yield of product into a given channel.

The IIC scenario may be viewed as the multichannel extension of the "laser-induced continuum structure" (LICS) phenomenon (see, for example, Knight *et al.*, 1990; Faucher *et al.*, 1993; Cavalieri *et al.*, 1998; and references therein). According to this view, the excitation by the ω_2 photon embeds an unpopulated bound state, $|E_{j_1}\rangle$, in the $|E, q, \mathbf{m}^-\rangle$ continuum. As a result, the continuum becomes structured while the $|E_{j_1}\rangle$ state becomes an unstable resonance. The structured continuum then interferes with the two-ω_1-photon dissociation of the populated state $|E_i\rangle$. The main new feature of the IIC theory presented below is the discovery that this interference effect may be of a different nature for different final channels.

A. Theory of Incoherent Interference Control

The equations governing the IIC scenario are most easily derived by treating both the light and the matter quantum-mechanically. The molecule, whose Hamiltonian is denoted by H_M, interacts with a quantized radiation field with radiative Hamiltonian H_R through the dipolar interaction term H_{MR}. The total Hamiltonian H is then given by

$$H = H_M + H_R + H_{MR} \equiv H_0 + H_{MR} \tag{112}$$

The photo-dissociation process is characterized, as for classical light, by a transition from $|E_i\rangle$, a bound eigenstate of H_M, to $|E, q, \mathbf{m}^-\rangle$, a continuum eigenstate of the same Hamiltonian, which, as in the classical field case, correlates in the infinite future with the noninteracting $|\epsilon_{\mathbf{m},q}\rangle|E - \epsilon_{\mathbf{m},q}\rangle$ product state.

When describing the radiation pulse, it is convenient to work with (multimode) number states $|N_k\rangle$, defined as the eigenstates of H_R,

$$H_R|N_k\rangle \equiv H_R|n_1^{(k)}, n_2^{(k)}, \ldots\rangle = \hbar \sum_l n_l^{(k)} \omega_l |N_k\rangle \equiv E_{N_k}|N_k\rangle \tag{113}$$

where E_{N_k} is the total radiation energy. The letters $k = i$ and f are used to label the initial and final states, respectively. The eigenstates of $H_0 \equiv H_M + H_R$ are a direct product of the molecular and photon states; e.g., $|(E, q, \mathbf{m}^-)N_f\rangle \equiv$

$|E, q, \mathbf{m}^-\rangle|N_f\rangle$. We call these states "partially" interacting because they encompass interaction via the material part of the Hamiltonian only.

The molecule-radiation interaction H_{MR} is given in the dipole approximation (Cohen-Tannoudji *et al.*, 1992) as

$$H_{MR} = -\mathbf{d} \cdot \epsilon, \quad \text{with} \quad \epsilon = i \sum_l \epsilon_l (\hat{\epsilon}_l a_l - \hat{\epsilon}_l^* a_l^\dagger) \tag{114}$$

where $\mathbf{d}$ is the electric dipole operator, ϵ is the amplitude of the radiation electric field, $\epsilon_l = (2\pi\hbar\omega_l/L^3)^{1/2}$, $\hat{\epsilon}_l$, ω_l are the polarization vector and angular frequency of mode l, respectively, and a_l, $a_l^\dagger$ are photon annihilation and creation operators.

The dynamics of photo-dissociation is completely described by the fully interacting state $|(E, q, \mathbf{m}^-), N_k^-\rangle$, which is an eigenstate of the total Hamiltonian H,

$$H|(E, q, \mathbf{m}^-), N_k^-\rangle = (E + E_{N_k})|(E, q, \mathbf{m}^-), N_k^-\rangle \tag{115}$$

The additional minus superscript on N_k indicates that the state $|(E, q, \mathbf{m}^-)N_k^-\rangle$ becomes the partially interacting state $|(E, q, \mathbf{m}^-)N_k\rangle$ when the radiative interaction H_{MR} is switched off. The $|(E, q, \mathbf{m}^-)N_k^-\rangle$ states satisfy an augmented Lippmann-Schwinger equation [whose purely material analogue is Eq. (26)] of the form

$$|(E, q, \mathbf{m}^-), N_k^-\rangle = |(E, q, \mathbf{m}^-), N_k\rangle + G(E^- + E_{N_k}) H_{MR} |(E, q, \mathbf{m}^-) N_k\rangle \tag{116}$$

where the resolvent $G(z) \equiv 1/(z - H)$.

If the system is initially in the partially interacting bound state $|E_i, N_i\rangle \equiv |E_i\rangle|N_i\rangle$, and the radiation-matter interaction is switched on suddenly, then the photo-dissociation amplitude to form the partially interacting state $|E, q, \mathbf{m}^-\rangle |N_f\rangle$ is given by $\langle (E, q, \mathbf{m}^-) N_f^- | E_i, N_i\rangle$. Because $\langle (E, q, \mathbf{m}^-) N_f | E_i, N_i\rangle = 0$, it follows from Eq. (116) that

$$\langle (E, q, \mathbf{m}^-), N_f^- | E_i, N_i\rangle = \langle (E, q, \mathbf{m}^-) N_f | H_{MR} G(E^+ + E_{N_f}) | E_i, N_i\rangle \tag{117}$$

Two quantities, derived from the $\langle (E, q, \mathbf{m}^-) N_f | H_{MR} G(E^+ + E_{N_f}) | E_i, N_i\rangle$ matrix elements, which can be computed numerically by a variety of techniques (Chen *et al.*, 1994, 1995; Shapiro and Bony, 1985; Balint-Kurti, 1986; Brumer and Shapiro, 1986b. Bandrauk *et al.*, 1989), are of interest: $P(E, q, N_f | E_i, N_i)$, the probability to obtain products in channel q at a given photon number state

distribution $\{N_f\}$ and total material energy E,

$$P(E,q,N_f|E_i,N_i) = \sum_{\mathbf{m}} |\langle (E,q,\mathbf{m}^-), N_f^- | H_{MR} G(E^+ + E_{N_f}) | E_i, N_i \rangle|^2 \quad (118)$$

and the total dissociation probability to channel q,

$$P(q) = \sum_{N_f} \int dE\, P(E,q,N_f|E_i,N_i) \quad (119)$$

Focusing on the case of a molecule in the presence of just two field modes, of electric field vectors ϵ_1 and ϵ_2 and frequencies ω_1 and ω_2, we can write the initial state as $|E_i,N_i\rangle = |E_i,n_1,n_2\rangle$, where n_1 and n_2 are the initial occupation numbers of the two field modes, and the molecule-radiation interaction H_{MR} as

$$H_{MR} = -\mathbf{d}\cdot\epsilon_1 - \mathbf{d}\cdot\epsilon_2 \quad (120)$$

The two frequencies are chosen such that $\hbar\omega_1 \approx E_{j_1} - E_i$, i.e., ω_1 is in resonance with the excitation frequency to state $|E_{j_1}\rangle$. ω_2 is chosen such that $E_i + 2\hbar\omega_1 \approx E_{j_2} + \hbar\omega_2$, which means that $2\hbar\omega_1 - \hbar\omega_2$ is in (2-1) resonance with the transition from $|E_i\rangle$ to $|E_{j_2}\rangle$ (see Fig. 1 for the application to Na_2).

Performing a perturbative expansion of Eq. (117) with H_{MR} as given in Eq. (120), and retaining the two lowest-order terms, we obtain that

$$\langle (E,q,\mathbf{m}^-), n_1-2, n_2 | H_{MR} G(E^+ + E_{N_f}) | E_i, n_1, n_2 \rangle = A + B + \cdots \quad (121)$$

$$A = \sum_{j_1 \neq i} \frac{\langle (E,q,\mathbf{m}^-), n_1 - 2 | \mathbf{d}\cdot\epsilon_1 | E_{j_1}, n_1 - 1\rangle \langle E_{j_1}, n_1 - 1 | \mathbf{d}\cdot\epsilon_1 | E_i, n_1\rangle}{\left(E^+ - E_{j_1} - \hbar\omega_1 - r_{j_1,j_1}\right)\left(E^+ - E_i - 2\hbar\omega_1 - r_{i,i}\right)} \quad (122)$$

$$B = \sum_{j_1,j_2(j_1\neq j_2\neq i)} \frac{\langle (E,q,\mathbf{m}^-), n_2 | \mathbf{d}\cdot\epsilon_2 | E_{j_2}, n_2 + 1\rangle r_{j_2,j_1} \langle E_{j_1}, n_1 - 1 | \mathbf{d}\cdot\epsilon_1 | E_i, n_1\rangle}{(E^+ - E_{j_2} - \hbar\omega_2 - r_{j_2,j_2})(E^+ - E_{j_1} - \hbar\omega_1 - r_{j_1,j_1})(E^+ - E_i - 2\hbar\omega_1 - r_{i,i})} \quad (123)$$

The r_{j_2,j_1} terms in Eq. (135), given by

$$r_{j_2,j_1} = \sum_{q',\mathbf{m}'} \int dE' \frac{\langle E_{j_2}, n_2 + 1 | \mathbf{d}\cdot\epsilon_2 | (E',q',\mathbf{m}'^-), n_2\rangle \langle (E',q',\mathbf{m}'^-), n_1 - 2 | \mathbf{d}\cdot\epsilon_1 | E_{j_1}, n_1 - 1\rangle}{E^+ - E'} \quad (124)$$

describe transitions between $|E_{j_1}\rangle$ and $|E_{j_2}\rangle$, accompanied by the absorption of one ω_1 photon and the stimulated emission of an ω_2 photon. Other sequential absorption and emission terms result from the higher-order contributions to Eq. (117).

The term A in Eq. (122) describes the direct resonant two-photon dissociation path $|E_i\rangle \rightarrow |E, q, \mathbf{m}^-\rangle$ via the intermediate states $|E_{j_1}\rangle$ (path A). The term B describes the dissociation path $|E_i\rangle \rightarrow |E', q', \mathbf{m}'^-\rangle \rightarrow |E_{j_2}\rangle \rightarrow |E, q, \mathbf{m}^-\rangle$ induced by ω_1 plus ω_2 (path B). It is important to note that the relative sign of the terms A and B depends on the frequency ω_2, resulting in a sensitivity of the final probability to the frequency of the control laser.

Equation (121) describes the photon fields by number states. However, a complete analysis of interference between the A and B paths necessitates an understanding of the role of the photon phase. Hence we sketch the same argument using multimode coherent states $|\alpha\rangle \equiv |\alpha_1\rangle \oplus |\alpha_2\rangle$, where $|\alpha_1\rangle$ and $|\alpha_2\rangle$ are coherent states of the ω_1 and ω_2 modes:

$$|\alpha_i\rangle = \sum_{n_i} \frac{\alpha_i^{n_i} \exp(-|\alpha_i|^2/2)}{\sqrt{n_i!}} |n_i\rangle, \quad i = 1, 2 \tag{125}$$

The quantity α_i is related to the average photon number $\bar{n}_i$ and to the phase ϕ_i of the ω_i laser as $\alpha_i = \sqrt{\bar{n}_i} \exp(i\phi_i)$.

Replacing Eq. (121) by $\langle \alpha | \langle E, \mathbf{m}^- | H_{MR} G(E^+ + E_{N_f}) | E_i \rangle | \alpha \rangle$ gives, within the rotating wave approximation,

$$\begin{aligned} \langle \alpha | \langle E, \mathbf{m}^- | H_{MR} G(E^+ + E_{N_f}) | E_i \rangle | \alpha \rangle &= e^{2i\phi_1} \bar{A} + e^{i\phi_2} e^{i(2\phi_1 - \phi_2)} \bar{B} + \cdots \\ &= e^{2i\phi_1} [\bar{A} + \bar{B} + \cdots] \end{aligned} \tag{126}$$

where $\bar{A}$ and $\bar{B}$ are of the same form as A and B in Eq. (121) but with the photon numbers n_1 and n_2 replaced by the average photon numbers $\bar{n}_1$ and $\bar{n}_2$. Hence, the leading terms in the dissociation probability $|\langle \alpha | \langle E, \mathbf{m}^- | H_{MR} G(E) | E_i \rangle | \alpha \rangle|^2$ can be obtained from Eq. (121) by replacing the photon numbers n_i by the average photon number $\bar{n}_i$. Most significantly, we see that the photodissociation probability is independent of the laser phase. Examination of the higher-order terms in the perturbative expansion of Eq. (117) (within the rotating wave approximation) shows a similar cancellation of the laser phase. Thus, the interference between path A and path B exists even for incoherent light.

Extensive control of the detailed and total probability to form a given q channel using this approach is demonstrated in the next subsection, where computations and experiments pertaining to Na_2 photo-dissociation are discussed. We note that in the actual calculations, it was in fact easier

to compute $\langle (E, q, \mathbf{m}^-), n_1 - 2, n_2 | H_{MR} G(E^+ + E_{N_f}) | E_i, n_1, n_2 \rangle$ [Eq. (117)] directly, using such methods as the high-field extension of the artificial channel method (Bandrauk and Atabek, 1989; Chen *et al.*, 1995; Shapiro and Bony, 1985) rather than the H_{MR} perturbative expansion. Note also that an alternative, complementary perspective on IIC has been advanced by Kobrak and Rice (1998a), based on photoselective adiabatic passage (Kobrak and Rice, 1998b). Their approach provides useful insights into incoherent interference control in the high-intensity limit and successfully reproduces the Na_2 results described below.

B. Computational and Experimental Demonstration

Incoherent interference control has been demonstrated both computationally and experimentally for the case of the two-photon dissociation of the Na_2 molecule. The photo-dissociation process we have examined is,

$$Na_2 \longrightarrow \begin{cases} Na(3s) + Na(3p) \\ Na(3s) + Na(4s) \\ Na(3s) + Na(3d) \end{cases} \tag{127}$$

The control objective is to produce preferentially the Na(3d) or Na(3p) product. In the IIC scenario this is done by varying one of the frequencies, either ω_1 or ω_2.

In the IIC experiment (Shnitman *et al.*, 1996) (see Fig. 10), two dye lasers pumped by a frequency-doubled Nd-Yag laser were used. One dye laser, whose frequency $\omega_2$was tuned between 13,312 cm^{-1} and 13,328 cm^{-1}, was used to dress the continuum with a $|E_{j_2}\rangle$ vib-rotational state of the $A^1\Sigma_u/^3\Pi_u$ electronic manifold (Chen *et al.*, 1993a). The other dye laser, whose frequency $\omega_1$was fixed at 17,474.12 cm^{-1}, was used to induce a two-photon dissociation of the $|E_{v=5,J=37}\rangle$ ground state of Na_2, through intermediate resonances (assigned as $v = 35$, $J = 38$ and $v = 35$, $J = 36$) of the $A^1\Sigma_u/^3\Pi_u$ manifold. The ω_1 and ω_2 pulses, both about 5 ns in duration with the stronger of them (ω_2) having an energy of ~3.5 mJ, were made to overlap in a heat pipe containing Na vapor at 370–410°C. Spontaneous emission from the excited Na atoms [Na(3d) → Na(3p) and Na(3p) → Na(3s)] resulting from the Na_2 photo-dissociation, was detected and dispersed in a spectrometer and a detector with a narrow-bandpass filter.

Figures 11 and 12 display the observed and computed Na(3d) and Na(3p) emission signal as a function of ω_2 at a fixed ω_1. We see that the computed and experimental results are in excellent agreement. Clearly, as the Na(3d) yield dips, the Na(3p) yield peaks, in accordance with theoretical calculations (Chen *et al.*, 1995). The controlled modulation of the Na(3p)/Na(3d)

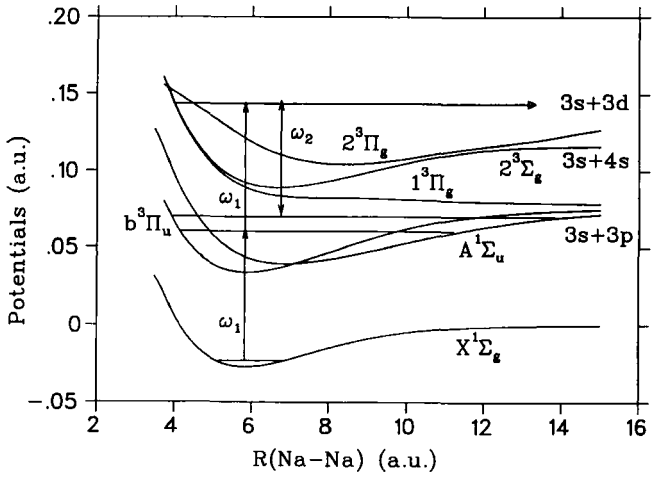

FIG. 10. Incoherent interference control (IIC) scheme and potential energy curves for Na_2. In this scheme a two-ω_1-photon excitation interferes with an ω_2 photon. The two-photon process proceeds from an initial state, assigned here as ($v = 5$, $J = 37$), via the $v = 35$, $J = 36, 38$ levels, belonging to the interacting $A^1\Sigma_u/^3\Pi_u$ electronic states, acting as intermediate resonances. The ω_2 photon dresses the continuum with the (initially unpopulated) $v = 93$, $J = 36$ and $v = 93$, $J = 38$ levels of the $A^1\Sigma_u/^3\Pi_u$ electronic states.

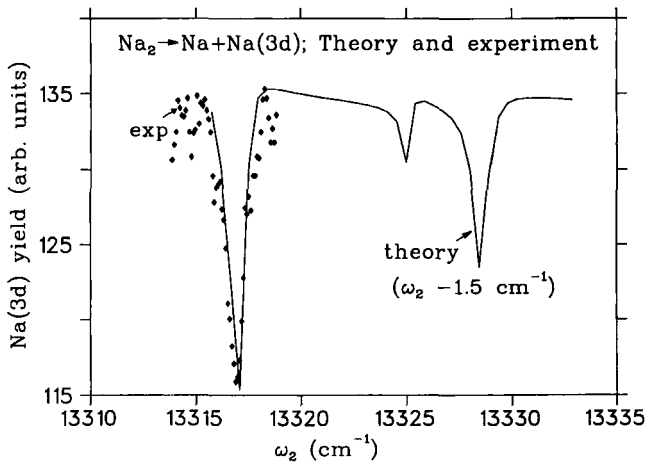

FIG. 11. Comparison of the experimental and theoretical $Na_2 \rightarrow Na(3s) + Na(3d)$ yields as a function of ω_2. In the calculation, an intermediate $v = 33$, $J = 31, 33$ resonance is used, and ω_1 is fixed at 17,720.7 cm^{-1}. The intensities of the two laser fields are $I(\omega_1) = 1.72 \times 10^8$ W/cm^2 and $I(\omega_2) = 2.84 \times 10^8$ W/cm^2. The ω_2 frequency axis of the calculated results was shifted by -1.5 cm^{-1} so that we could better compare the predicted and measured lineshapes.

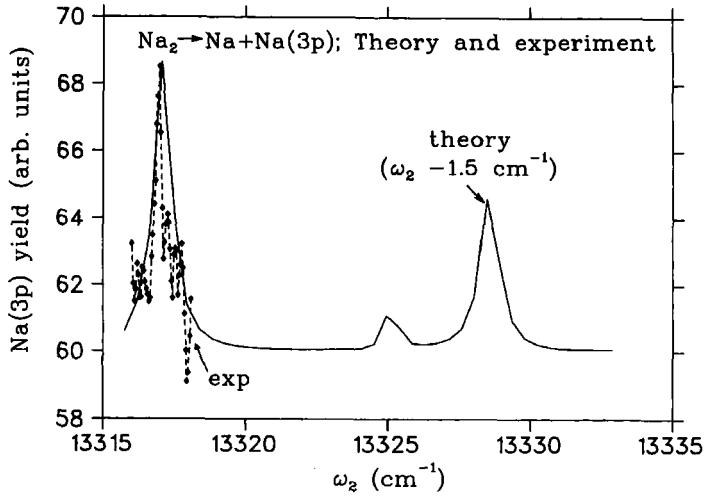

FIG. 12. Comparison of the experimental and theoretical $Na_2 \rightarrow Na(3s) + Na(3p)$ yields as a function of ω_2, with parameters as in Fig. 11.

branching ratio is seen to exceed 30%. It is important to note that this degree of experimental control was attained in a rather hostile environment, i.e., a heat pipe with ongoing molecular collisions, and using lasers with only partially coherent light.

VII. Coherent Control of Bimolecular Processes

The results discussed above deal with control of unimolecular processes, i.e., processes that begin with a single molecule that subsequently undergoes excitation and dynamics. Control has been described in two interlinked stages: (a) the use of multiple excitation routes to create controllable superposition states in the continuum and (b) the effect of the controllable interference term on the final outcome of the process. In this section we generalize coherent control to bimolecular collision processes, i.e., collisions of the type

$$A + D \rightarrow F + G \tag{128}$$

where A, D, F, G are, in general, molecules. Here F and G can be identical to A and D (nonreactive scattering) or different from A and D (reactive scattering). Unlike unimolecular processes, we first demonstrate that coherent control is possible in bimolecular scattering if one creates a superposition of energetically

degenerate scattering states; then we discuss methods for experimentally preparing such states.

Consider then Eq. (128), where we label $A + D$ as arrangement q and $F + G$ as arrangement q'. Below we focus on atom (A) plus diatom ($D = B - C$) scattering, although the results are easily generalized to polyatomic scattering. Eigenfunctions of the asymptotic Hamiltonian, where $A + D$ are widely separated are given, in accordance with Eq. (18), by $|E, q, \mathbf{m}; 0\rangle$, where we have made the channel label q explicit. States of the product are similarly denoted $|E, q', \mathbf{n}; 0\rangle$, and $|E, q', \mathbf{n}^-\rangle$ denotes the incoming solutions associated with product in $|E, q', \mathbf{n}; 0\rangle$. The probability $P_E(\mathbf{n}, q'; \mathbf{m}, q)$ of forming $|E, q', \mathbf{n}; 0\rangle$, having initiated the scattering in $|E, q, \mathbf{m}; 0\rangle$, is given by (Taylor, 1972) as

$$P_E(\mathbf{n}, q'; \mathbf{m}, q) = |\langle E, q', \mathbf{n}; 0 | S | E, q, \mathbf{m}; 0\rangle|^2 \tag{129}$$

where S is the scattering matrix. In analogy with Eq. (36), one can rewrite the probability in terms of $\langle E, q, \mathbf{n}^- | V_q | E, q, \mathbf{m}; 0\rangle$, where V_q is defined, in analogy with Eq. (14), as the component of the total potential that vanishes as the distance A to D becomes arbitrarily large. It is traditional in scattering theory, however, to compute the cross section, given by

$$\sigma_E(\mathbf{n}, q'; \mathbf{m}, q) = |\langle E, q', \mathbf{n}^- | V_q | E, q, \mathbf{m}; 0\rangle|^2 \tag{130}$$

rather than the probability. In addition to the above state-to-state cross section, the cross section of forming product in arrangement q' independent of the internal state $\mathbf{n}$,

$$\sigma_E(q'; \mathbf{m}, q) = \sum_{\mathbf{n}} |\langle E, q', \mathbf{n}^- | V_q | E, q, \mathbf{m}; 0\rangle|^2 \tag{131}$$

is also of interest. Assorted other cross sections may be defined, depending upon which of the elements of $\mathbf{n}$ are summed over. Of relevance below are (a) $\sigma_E(q', \theta, \phi; \mathbf{m}, q)$, corresponding to scattering into the q' product channel and into scattering angles (θ, ϕ), and (b) the traditional differential cross section $\sigma_E(q', \theta; \mathbf{m}, q) = \int d\phi \, \sigma_E(q', \theta, \phi; \mathbf{m}, q)$.

In order to control bimolecular cross sections, we now consider scattering from an initial *superposition* state $|E, q, \{c_\mathrm{m}\}\rangle$ comprised of N energetically degenerate states $|E, q, \mathbf{m}; 0\rangle$:

$$|E, q, \{c_\mathrm{m}\}\rangle = \sum_{\mathrm{m}=1}^{N} c_\mathrm{m} |E, q, \mathbf{m}; 0\rangle \tag{132}$$

The cross section associated with using Eq. (132) as the initial state, obtained by substituting Eq. (132) in Eq. (130), is

$$\begin{aligned}\sigma_E(\mathbf{n}, q'; \{c_m\}, q) &= |\langle E, q', \mathbf{n}^- | V_q \sum_m c_m | E, q, \mathbf{m}; 0\rangle|^2 \\ &= \sum_m |c_m|^2 \langle E, q', \mathbf{n}^- | V_q | E, q, \mathbf{m}; 0\rangle|^2 \\ &\quad + \sum_{m'} \sum_{m \neq m'} c_m c_{m'}^* \langle E, q', \mathbf{n}^- | V_q | E, q, \mathbf{m}; 0\rangle \\ &\quad \times \langle E, q, \mathbf{m}'; 0 | V_q | E, q', \mathbf{n}^-\rangle \\ &\equiv \sum_m |c_m|^2 \sigma(\mathbf{n}, q'; \mathbf{m}, q) + \sum_{m'} \sum_{m \neq m'} c_m c_{m'}^* \sigma(\mathbf{n}, q'; \mathbf{m}', \mathbf{m}, q)\end{aligned} \tag{133}$$

where $\sigma(\mathbf{n}, q'; \mathbf{m}', \mathbf{m}, q)$ is defined via Eq. (133). The total cross section is given by

$$\sigma_E(q'; \{c_m\}, q) = \sum_n \sigma_E(\mathbf{n}, q'; \{c_m\}, q) \tag{134}$$

Note that Eq. (133) and hence Eq. (134) are now of the standard coherent control form, i.e., direct contributions from each member of the superposition, proportional to $|c_m|^2$, plus interference terms that are proportional to $c_m c_{m'}^*$. Hence, by controlling the c_m, we can control the scattering cross section. Note also that both the direct and the interference amplitudes are composed of the same amplitudes. As such, we can even expect control to be effective far from the onset of reaction at reaction thresholds, a feature that overcomes the limitations of previously proposed bimolecular control methods (Krause *et al.*, 1990).

A. Degenerate e_M Superpositions

The easiest way of implementing bimolecular control in the lab is to start with a superposition of scattering states having the same incoming translational wave function $|\mathbf{k}_m\rangle$. This means, however, by Eq. (132), that in order to maintain the degeneracy of the total continuum energy E, we must build the superposition state from degenerate internal states $|e_m\rangle$:

$$|E, q, \{c_m\}\rangle = \sum_m c_m |E, q, \mathbf{m}; 0\rangle \equiv |\mathbf{k}_m\rangle \sum_m c_m |e_m\rangle \tag{135}$$

In atom-diatom scattering, the most obvious candidate for degenerate $|e_m\rangle$ are the $|J, M_J\rangle$ states associated with fixed diatomic rotational angular momentum J. However, in this case the interference terms $\sigma(\mathbf{n}, q'; \mathbf{m}', \mathbf{m}, q)$ contain the cylindrically asymmetric $\exp[i(M_J - M'_J)\phi]$ factors (Abrashkevich *et al.*, 1999), which average out upon integration over the azimuthal angle ϕ. As a result, although control over the fully differential $\sigma_E(q', \theta, \phi; \{c_m\}, q)$ cross section is possible, control over the ϕ-averaged differential cross section $\sigma_E(q', \theta; \{c_m\}, q)$ and the total cross section $\sigma_E(q'; \{c_m\}, q)$ cannot be achieved in this way.

To examine the extent of control afforded in this way, we performed detailed computations on one of the most widely studied prototype exchange reactions, that of

$$D + H_2 \rightarrow H + HD$$

Our computations were carried out for $E = 1.25$ eV and H_2 in the $v = 0, J = 2$ vib-rotational state. Both the reactive and the nonreactive differential cross sections $a + \phi = 0$ [denoted $\sigma^R(\theta)$ and $\sigma^{NR}(\theta)$] were examined. Figure 13 shows $\sigma^R(\theta)/\sigma^{NR}(\theta)$ for the linear superposition $c_1|E, J, \kappa_1 = 2\rangle + c_2|E, J, \kappa_2 = 0\rangle$ for various values of $s = |c_1|^2/[|c_1|^2 + |c_2|^2]$ with $\phi_{12} = \arg(a_2/a_1) = 157°$. Here $s = 0$ corresponds to scattering out of the initial state $v = 0, J = 2, \kappa = 2$; and $s = 1$ corresponds to scattering from $v = 0, J = 2, \kappa = 0$. The ratio of controlled differential cross sections is seen to be considerably different from the uncontrolled ratio. For example, the controlled $\sigma^R(\theta)/\sigma^{NR}(\theta)$ at $\theta = 91°$ at $s = 0.748$ is approximately twice as large as the uncontrolled ratios. Analysis of Fig. 13 shows that the maxima and minima of the controlled ratio in the region between 50° and 120° are positioned at the corresponding minima and maxima of the uncontrolled ratios. Exactly the opposite behavior is seen in the outer regions of θ. Hence, coherent control changes both the magnitude and the structure of the differential cross section.

Results for the ratio of the reactive versus nonreactive cross sections at a fixed 0, J value are shown in Fig. 14 for scattering from $c_i|v = 0, J = 2, \kappa = 2\rangle + c_2|v = 0, J = 2, \kappa = 1\rangle$, as a function of the control parameters ϕ_{12} and s. The ratio is seen to vary from 0.032 to 0.113, showing maxima and minima that are well outside the range of results for scattering from a single κ state.

This approach can be extended to include all available energetically degenerate κ_i states ($\kappa_i = -J, -J + 1, \ldots, J$), with concomitant improvement in the ratio of reactive to nonreactive product. In addition, one can optimize this ratio (Abrashkevich *et al.*, 1999) as a function of the coefficients c_m. For the $J = 2$ case, the maximum $\sigma^R/\sigma^{NR} = 0.143$, a 20% improvement over the results for a superposed pair of κ_i states.

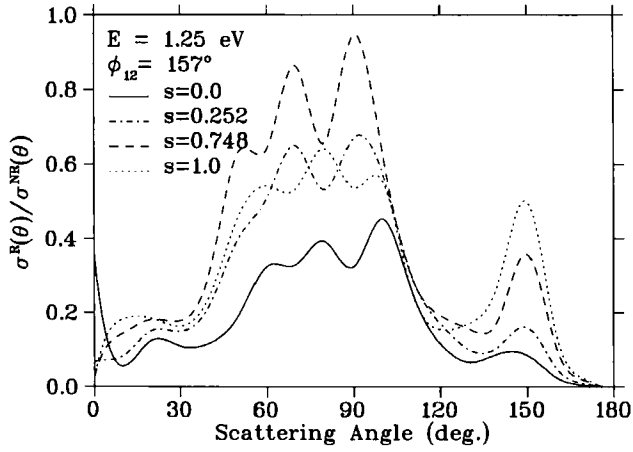

FIG. 13. Dependence of the ratio of the reactive to nonreactive differential cross section $\sigma^R(\theta)/\sigma^{NR}(\theta)$ in controlled D + H_2 on the scattering angle θ at $\phi_{12} = 157°$ for four values of s: $s = 0, 1, 0.252$, and 0.748. (From Abrashkevich *et al.*, 1998a.)

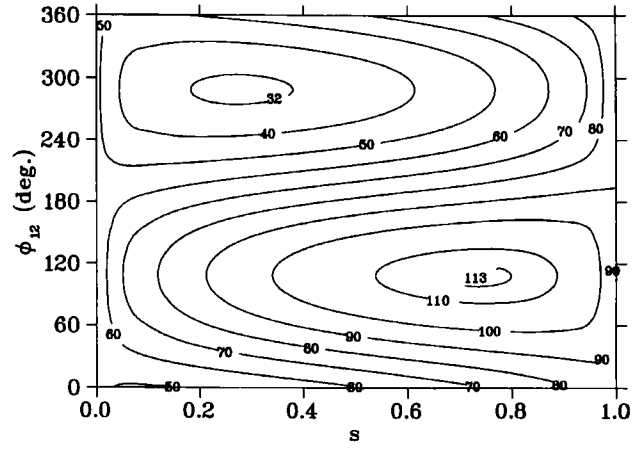

FIG. 14. Contour plot of the ratio of reactive to nonreactive cross section σ^R/σ^{NR} ($\times 10^3$) in controlled D + H_2 as a function of ϕ_{12} and s, at a fixed 0, J value.

It remains to ask how such a superposition of helicity states may be prepared. One possibility is a precursor step consisting of the coherently controlled photo-dissociation of a molecule to produce a diatomic product in a controlled superposition of κ states relative to an incoming partner. For example, in the D + H_2 case we can subject H_2S to a coherently controlled photo-dissociation step to produce H_2 in a superposition such that aiming the

D atom exactly antiparallel to the direction of the H_2 motion will produce the desired initial $|E, q, \{c_m\}\rangle$.

B. Sculpted Imploding Waves

Rather than using a superposition of internal states $|e_m\rangle$, as in the above discussion, it is possible to effect bimolecular control by using a superposition of translational wavefunctions $|\mathbf{k}_m\rangle$ (Frishman *et al.*, 1999). In order to examine a superposition of incident plane waves, we first perform a partial-wave decomposition of each of the plane waves, assumed directed along the Z-axis:

$$\begin{aligned}\langle \mathbf{R}|\mathbf{k}_m\rangle &= \exp(i\mathbf{k}_m \cdot \mathbf{R}) = \exp(ik_m Z) = \exp(ik_m R\cos\theta) \\ &= \sum_l c_l j_l(k_m R) P_l(\cos\theta) \end{aligned} \tag{136}$$

where $c_l = i^l(2l+1)$ and $j_l(k_m R), P_l(\cos\theta)$ are the spherical Bessel function and Legendre polynomial, respectively. We see that each incoming plane wave is in fact a superposition of energetically degenerate states with fixed coefficients c_l. This suggests the possibility of altering the c_l to produce modified states $\langle \mathbf{R}|\mathbf{k}_{mod}\rangle$ that will display different quantum interferences, hence altering the product cross sections. Thus, in this instance, the initial $|E, q, \{c_m\}\rangle$ is given by $|E, q, \{c_m\}\rangle = |e_m\rangle|\mathbf{k}_{mod}\rangle$, where $|\mathbf{k}_{mod}\rangle$, a "sculpted incoming wavepacket," is parametrized by coefficients $\{c_l\}$.

The effect of changing the structure of the incident wavepacket cannot, however, be measured using the standard definition of the cross section, because that definition relies on a constant flux from one direction (Taylor, 1972). Rather, we consider the magnitude of $F_{q'}$, the outgoing flux into the product channel, as a function of the $|c_l|$, with the constraint that the incident wavefunction is normalized to the usual Dirac delta function (for alternative choices of constraints, see Frishman *et al.*, 1999).

As an example of the control afforded by this approach, consider rotational excitation in a model of the $Ar + H_2(J, M_J) \rightarrow Ar + H_2(J'M_{J'})$ collision. Optimizing the phases χ_l of $c_l = |c_l|\exp(i\chi_l)$ allows a direct study of the effect of varying the interferences between partial-wave components on $F_{q'}$. Typically, altering χ_l allowed for considerable control. For example, with $J = 2, M_J = 0, J' = 0$, it was possible to change $F_{q'}$ by two orders of magnitude, from 5.1×10^{-4} to 3.8×10^{-2}, just by varying the χ_l. These values are to be compared to $F_{q'} = 1 \times 10^{-2}$ associated with scattering from an incident plane wave. Real and imaginary parts of the incident wave functions leading to these maximum and minimum values of the outgoing flux are

shown in Fig. 15. They are distinctly different from one another and from a plane wave.

It remains to establish viable methods to prepare such sculpted imploding matter waves experimentally. Once again, we anticipate doing so via a

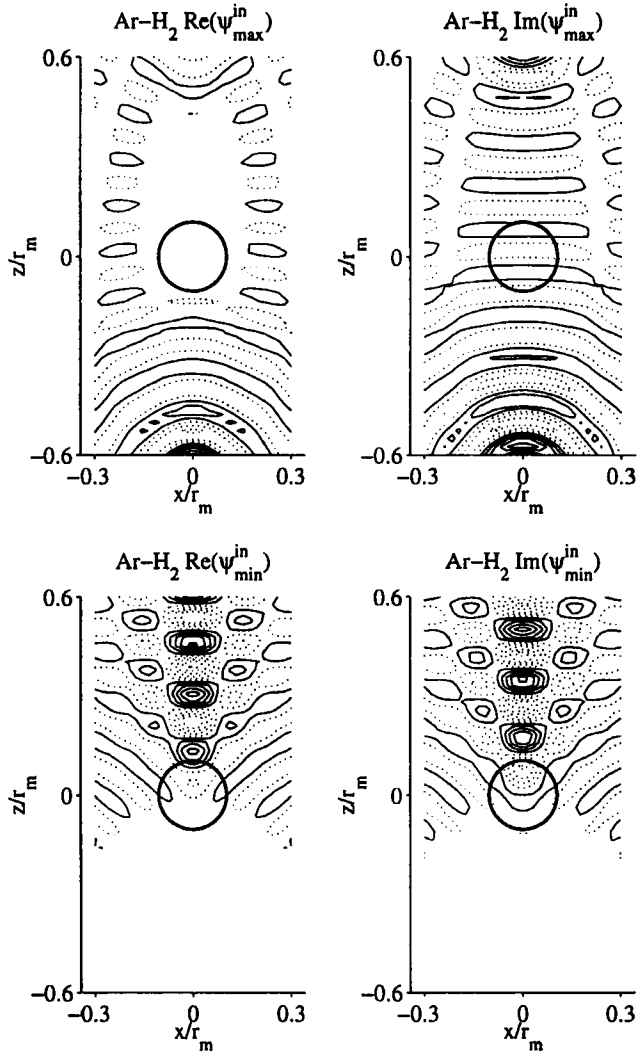

FIG. 15. Real and imaginary parts of the incident wave function leading to maximum and minimum outgoing flux for $Ar + H_2(v = 0,\ j = 2,\ m_j = 0)$. (From Frishman *et al.*, in preparation.)

pre-reactive photo-dissociation step, possibly in conjunction with matter interferometry techniques.

C. Optimized Bimolecular Scattering: Enhancement and Total Suppression

We now extend the treatment of Section VII.A to the case of a superposition composed of more than two states. On the basis of Eqs. (130) and (131), we introduce in this subsection a scheme that optimizes $\sigma(q';\{c_m\},q)$ or $\sigma(q',\mathbf{n};\{c_m\},q)$ as a function of c_m for an arbitrary number of states. One of the most interesting outcomes of this procedure is that it leads to a strong analytic result: if the number of initial open states in the reactant space exceeds the number of open states in the product space, it is possible to find a particular set of $\{c_m\}$ such that one can totally *suppress* reactive scattering. This result is proven below and applied to display the total suppression of tunneling (Frishman *et al.*, 1998).

Consider scattering from incident state $|E,q,\mathbf{n};0\rangle$ to final state $|E,q',\mathbf{m};0\rangle$. To simplify the notation, we specialize the treatment to the case where the $\mathbf{m}$ and $\mathbf{n}$ labels pertain to just a single quantum number, denoted i and f, with associated free states $|E,q,i;0\rangle$ and $|E,q',f;0\rangle$. In accordance with Eq. (129), the probability $P(f,q';i,q)$ of producing product in final state $|f,E,q'\rangle$, having started in the initial state $|i,E,q\rangle$, is

$$P(f,q';i,q) = |S_{fi}|^2 \tag{137}$$

where $S_{fi} = \langle E,f,q'|S|E,i,q\rangle$ and where S is the scattering matrix for the process. The total probability $P(q';i,q)$ of scattering into arrangement channel q', assuming m open product states, is given by

$$P(q';i,q) = \sum_{f=1}^{m} |S_{fi}|^2 \tag{138}$$

To simplify the notation, we have not carried an E label in the probabilities: fixed energy E is understood.

If we now consider scattering from an initial state $|E,q,\{c_i\}\rangle$ comprised of a linear superposition of k states, [i.e., Eq. (146) with $N=k$]. Then the probability of forming $|E,q',f\rangle$ from this initial state is

$$P(f,q';\mathbf{c},q) = \left|\sum_{i=1}^{k} c_i S_{fi}\right|^2 \tag{139}$$

and the total reactive scattering probability into channel q', $P(q';\mathbf{c},q)$, is

$$P(q';\mathbf{c},q)=\sum_{f=1}^{m}\left|\sum_{i=1}^{k}c_iS_{fi}\right|^2 \tag{140}$$

To simplify the notation, we introduce the matrix $\sigma=\mathbf{S}_{q'}^{\dagger}\mathbf{S}_{q'}$ with elements $\sigma_{ij}=\sum_{f=1}^{m}S_{fj}^{*}S_{fi}$, which allows us to rewrite Eq. (140) as

$$P(q';\mathbf{c},q)=\mathbf{c}^{\dagger}\sigma\mathbf{c} \tag{141}$$

Here † denotes the Hermitean conjugate, and the q' subscript on the $\mathbf{S}$ indicates that we are dealing with the submatrix of the S matrix associated with scattering into product channel q'.

One can optimize scattering into arrangement channel q', with the normalization constraint $\sum_{i=1}^{k}|c_i|^2=1$, by requiring

$$\frac{\partial}{\partial c_k^{*}}\left[P(q';\mathbf{c},q)-\lambda\sum_{i=1}^{k}|c_i|^2\right]=\frac{\partial}{\partial c_k^{*}}[\mathbf{c}^{\dagger}\sigma\mathbf{c}-\lambda\mathbf{c}^{\dagger}\mathbf{c}]=0 \tag{142}$$

where λ is a Lagrange multiplier. Explicitly taking the derivative gives the result that the optimized coefficients $\mathbf{c}_\lambda$ satisfy the eigenvalue equation

$$\sigma\mathbf{c}_\lambda=\lambda\mathbf{c}_\lambda \tag{143}$$

Additional labels may be necessary to account for degeneracies of the eigenvectors $\mathbf{c}_\lambda$.

We first note that if $\lambda=0$ is an eigenvalue of Eq. (143) with eigenfunctions $\mathbf{c}_0$, then by inserting Eq. (143), into Eq. (141) we have that $P(q';\mathbf{c}_0,q)=0$. That is, if $\lambda=0$ is a solution to Eq. (143), then the coefficients $\mathbf{c}_0$ completely suppress reaction into arrangement channel q'.

Clearly, $\lambda=0$ is a solution if

$$\det(\sigma)=\det(\mathbf{S}_q'^{\dagger}\mathbf{S}_q')=0 \tag{144}$$

which is the case if the number of initial states k participating in the initial superposition is greater than the number m of open product states, a situation that invariably occurs for endoergic processes. To see this result, note that under these circumstances, σ is a matrix of order $k\times k$ and $\mathbf{S}_{q'}$ is of order $k\times m$. If $k>m$, we can construct a $k\times k$-order matrix $\mathbf{A}_q'$ by adding a submatrix of

$(k-m)$ rows of zeros to the lower part of $\mathbf{S}_{q'}$. Then

$$\det(\sigma) = \det(\mathbf{S}_{q'}^{\dagger}\mathbf{S}_{q'}) = \det(\mathbf{A}_{q'}^{\dagger}\mathbf{A}_{q'}) = \det(\mathbf{A}_{q'}^{\dagger})\det(\mathbf{A}_{q'}) = 0 \qquad (145)$$

The last equality holds because the determinants of $\mathbf{A}_{q'}$ and $\mathbf{A}_{q'}^{\dagger}$ are zero.

As an example of the kind of results that are possible, consider the optimization of a barrier penetration problem modeled by a set of multichannel Schrödinger equations of the type

$$\Psi''(r) = -\frac{2\mu}{\hbar^2}(\mathbf{E}-\mathbf{V})\Psi(r) \qquad (146)$$

where μ is the relevant mass, $\mathbf{V}$ is the potential matrix, $\mathbf{E}$ is a diagonal matrix with elements $E-e_i$, and k is the total number of open channels in arrangement q. Sample scattering results for $k=4$ using a potential matrix constructed from Eckart potentials, i.e.,

$$V_{i\ell}(r) = -\frac{a_{i\ell}\xi}{1-\xi} - \frac{b_{i\ell}\xi}{(1-\xi)^2} + c_{i\ell}, \quad i,\ell = 1,\ldots,4 \qquad (147)$$

where $\xi = -\exp(2\pi r/t)$, with t a distance potential parameter, are shown in Fig. 16. Reactivity is shown as a function of energy for the case where the number of populated initial states j is less than k; here $j=3$. The curves labeled P_i correspond to the standard $P(q';i,q)$, i.e., total reaction probability from each of the individual initial states. The quantities P_1 and P_3, which are open asymptotically at all energies, show a gradual rise with increasing energy, whereas P_2, which is closed on the product side until $E_{th}(3) = 0.008$ a.u., stays rather small until $E = E_{th}(3)$, where it displays a very rapid rise to near unity. Total reaction probability reaches unity above $E_{th}(4) = 0.010$ a.u., the threshold for the opening of the fourth channel.

Of particular relevance here are the solid curves in Fig. 16, which show the maximum and minimum reactivity obtained from the optimal solutions to Eq. (143). The maximum reactivity is seen to be substantially larger than any of the individual P_i and to reach unity at significantly lower energies than any of these solutions. Minimal reactivity, as predicted by the argument presented above, is seen to be zero for $E < E_{th}(3)$ because the total number of states $(j=3)$ in the superposition exceeds the number of open product states $(m=2)$. At $E > E_{th}(3)$ a third product channel opens so that $j=m$ and the minimal solution is no longer zero.

Note also that the minimum reactivity curve in Fig. 16 reflects a variety of different interesting behaviors, depending on the particular energy. Specifically, below the maximum of V_{11} at 0.005 a.u., the zero minimum corresponds

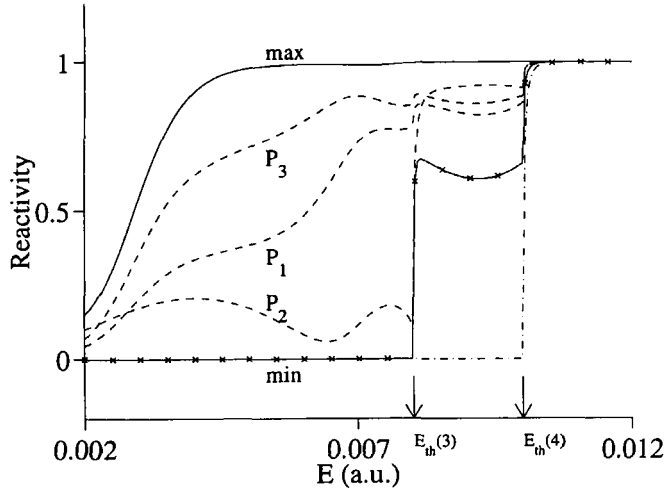

FIG. 16. Reactivity shown as a function of energy in a model system. Dashed curves labeled P_i correspond to the total reactivity from each of the three individual initial states in the prepared superposition. Solid curves with crosses denote the reactivity obtained by solving Eq. (143) for the optimal solutions. The two arrows indicate the threshold energies for opening of the third and fourth channels. The dot-dash curve shows the minimum reactivity resulting from a separate computation that includes four states in the initial superposition.

to suppression of tunneling through that barrier. Above 0.005 a.u., the zero minimum corresponds to suppression of the reactive scattering that occurs *above* the barrier.

Thus it is clear that the ability to superimpose degenerate scattering states has great potential for the control of scattering processes. Note also that, as an obvious extension, similar results hold for tunneling in bound systems if the total number of initial degenerate states at the energy of interest exceeds the number of accessible final states at that energy.

VIII. Summary

Coherent control has been demonstrated formally, computationally, and experimentally to be a viable method for controlling the outcome of isolated atomic molecular and electronic processes that form products in the continuum. It is a method that takes advantage of the quantum nature both of matter and of the incident light to encode quantum interference information into the molecular dynamics. That is, molecular reaction dynamics is intimately linked to the wavefunction phases that are controllable through coherent optical phase excitation. The result is a powerful method to control the dynamics of atomic, molecular, and electronic processes.

IX. Acknowledgments

We are grateful to the U.S. Office of Naval Research for support of the vast majority of this research.

X. References

Abrashkevich, A., Brumer, P., and Shapiro, M. (1999). In preparation.
Abrashkevich, A., Shapiro, M., and Brumer, P. (1998a). *Phys. Rev. Lett.* 81, 3789.
Abrashkevich, D., Shapiro, M., and Brumer, P. (1998b). *J. Chem. Phys.* 108, 3585.
Asaro, C., Brumer, P., and Shapiro, M. (1988). *Phys. Rev. Lett.* 60, 1634.
Assion, T., Baumert, T., Bergt, M., Brixner, T., Kiefer, B., Seyfried, V., Strehle, M., and Gerber, G. (1998). *Science* 282, 919.
Balint-Kurti, G. G., and Shapiro, M. (1981). *Chem. Phys.* 61, 137.
Balint-Kurti, G. G., and Shapiro, M. (1986). *Adv. Chem. Phys.* 60, 403.
Bandrauk, A. D., and Atabek, O. (1989). *Adv. Chem. Phys.* 73, 823.
Bandrauk, A. D., Gauthier, J.-M., and McCann, J. F. (1992). *Chem. Phys. Lett.* 200, 399.
Baranova, B. A., Chudinov, A. N., and Ya Zel'dovitch, B. (1990). *Opt. Comm.* 79, 116.
Bardeen, C. J., Yakovlev, V. V., Wilson, K. R., Carpenter, S. D., Weber, P. M., and Warren, W. S. (1997). *Chem. Phys. Lett.* 280, 151.
Barron, L. D. (1982). *Molecular light scattering and optical activity.* Cambridge University Press (Cambridge, UK).
Barron, L. D. (1986). *Chem. Soc. Rev.* 15, 189.
Baumert, T., Grosser, M., Thalweiser, R., and Gerber, G. (1991). *Phys. Rev. Lett.* 67, 3753.
Brumer, P., and Shapiro, M. (1986a). *Chem. Phys. Lett.* 126, 541.
Brumer, P., and Shapiro, M. (1986b). *Adv. Chem. Phys.* 60, 371.
Brumer, P., and Shapiro, M. (1992). *Ann. Rev. Phys. Chem.* 43, 257.
Cavalieri, S., Eramo, R., and Fini, L. (1997). *Phys. Rev. A* 55, 2941.
Cavalieri, S., Eramo, R., Fini, L., Materazzi, M., Faucher, O., and Charalambidis, D. (1998). *Phys. Rev. A* 57, 2915.
Chan, C. K., Brumer, P., and Shapiro, M. (1991). *J. Chem. Phys.* 94, 2688.
Charron, E., Guisti-Suzor, A., and Mies, F. H. (1993). *Phys. Rev. Lett.* 71, 692.
Charron, E., Giusti-Suzor, A., and Mies, F. H. (1995). *Phys. Rev. Lett.* 75, 2815.
Chelkowski, S., and Bandrauk, A. D. (1991). *Chem. Phys. Lett.* 186, 284.
Chen, C., Yin, Y.-Y., and Elliott, D. S. (1990). *Phys. Rev. Lett.* 64, 507; *Phys. Rev. Lett.* 65, 1737.
Chen, Z., Shapiro, M., and Brumer, P. (1993a). *J. Chem. Phys.* 98, 6843.
Chen, Z., Shapiro, M., and Brumer, P. (1993b). *J. Chem. Phys.* 98, 8647.
Chen, Z., Shapiro, M., and Brumer, P. (1994). *Chem. Phys. Lett.* 228, 289.
Chen, Z., Shapiro, M., and Brumer, P. (1995). *J. Chem. Phys.* 102, 5683.
Cohen-Tannoudji, C., J. Dupont-Roc, J., and G. Grynberg, G. (1992). *Atom-photon interactions.* Wiley (New York).
Dupont, E., Corkum, P. B., Liu, H. C., Buchanan, M., and Wasilewski, Z. R. (1995). *Phys. Rev. Lett.* 74, 3596.
Faucher, O., Charalambidis, D., Fotakis, C., Zhang, J., and Lambropoulos, P. (1993). *Phys. Rev. Lett.* 70, 3004.
Frishman, E., Shapiro, M., and Brumer, P. (1998). *J. Chem. Phys.* In press.
Frishman, E., Shapiro, M., and Brumer, P. (1999). In preparation.
Gordon, R. J., and Rice, S. A. (1997). 48, 595.

Hache, A., Kostoulas, Y., Atanasov, R., Hughes, J. L. P., Sipe, J. E., and van Driel, H.M. (1997). *Phys. Rev. Lett.* 78, 306.
Hammerich, A. D., Manthe, U., Kosloff, R., Meyer, H. D., and Cederbaum, L. S. (1994). *J. Chem. Phys.* 101, 5623.
Hollas, J. M. (1982). *High resolution spectroscopy.* Butterworths (London).
Ivanov, M. Y., Corkum, P. B., and Dietrich, P. (1993). *Laser Physics* 3, 375.
Ivanov, M., Corkum, P. B., Zuo, T., and Bandrauk, A. (1995). *Phys. Rev. Lett.* 74, 2933.
Jakubetz, W., Manz, J., and Schreier, H. J. (1990). *Chem. Phys. Lett.* 165, 100.
Jiang, X.-P., and Brumer, P. (1991). *J. Chem. Phys.* 94, 5833; *Chem. Phys. Lett.* 180, 222.
Jiang, X.-P., Shapiro, M., and Brumer, P. (1996). *J. Chem. Phys.* 104, 607.
Kleiman, V. D., Zhu, L., Li, X., and Gordon, R. J. (1995). *J. Chem. Phys.* 102, 5863.
See, for example, Knight, P. L., Lauder, M. A., and Dalton, B. J. (1990). *Phys. Rep.* 190, 1.
Kobrak, M. N., and Rice, S. A. (1998a). *J. Chem. Phys.* 109, 1.
Kobrak, M. N., and Rice, S. A. (1998b). *Phys. Rev. A* 57, 2885.
Kohler, B., Krause, J. L., Raski, F., Wilson, K. R., Yakovlev, V. V., Whitnell, R.M., and Yan, Y. (1995). *Acct. Chem. Res.* 28, 133.
Kosloff, R. (1988). *J. Phys. Chem.* 92, 2087.
Kosloff, R. (1994). *Ann. Rev. Phys. Chem.* 45, 145.
Kosloff, R., Rice, S. A., Gaspard, P., Tersigni, S., Tannor, and D. J. (1989). *Chem. Phys.* 139, 201.
Krause, J., Shapiro, M., and Brumer, P. (1990) *J. Chem. Phys.* 92, 1126.
Krause, J. L., Whitnell, R. M., Wilson, K. R., Yan, Y., and Mukamel, S. (1993). *J. Chem. Phys.* 99, 6562.
Leforestier, C., Bisseling, R., Cerjan, C., Feit, M., Friesner, R., Guldberg, A., Hammerich, A. D., Julicard, G., Karrlein, W., Dieter Meyer, H., Lipkin, N., Roncero, O., and Kosloff, R. (1991). *J. Comp. Phys.* 94, 59.
Levine, R. D. (1969). *Quantum mechanics of molecular rate processes.* Clarendon (Oxford, UK).
Lu, S.-P., Park, S. M., Xie, Y., and Gordon, R. J. (1992). *J. Chem. Phys.* 96, 6613.
Manolopoulos, D. E., D'Mello, M., and Wyatt, R. E. (1991). *J. Chem. Phys.* 93, 403.
Muller, H. G., Bucksbaum, P. H., Schumacher, D. W., and Zavriyev, A. (1990). *J. Phys. B* 23, 2761.
Park, S. M., Lu, S.-P., and Gordon, R. J. (1991). *J. Chem. Phys.* 94, 8622.
Peirce, A. P., Dahleh, M. A., and Rabitz, H. (1988). *Phys. Rev. A* 37, 4950; *ibid.* (1990). 42, 1065, Shi, S., and Rabitz, H. (1991). *Comp. Phys. Comm.* 63, 71.
Potter, E. D., Herek, J. L., Pedersen, S., Liu, Q., and Zewail, A. H. (1992). *Nature* 355, 66.
Potvliege, R. M., and Smith, P. H. G. (1992). *J. Phys. B* 25, 2501.
Pratt, S. T. (1996). *J. Chem. Phys.* 104, 5776.
Schafer, K. J., and Kulander, K. C. (1992). *Phys. Rev. A* 45, 8026.
Schmidt, I. (1987). Ph.D. Thesis, Kaiserslautern University.
Schubert, M., and Wilhelmi, B. (1986). *Nonlinear optics and quantum electronics.* Wiley (New York).
Segev, E., and Shapiro, M. (1982). *J. Chem. Phys.* 77, 5604.
Seideman, T., Shapiro, M., and Brumer, P. (1989). *J. Chem. Phys.* 90, 7132.
Shapiro, M. (1993). *J. Phys. Chem.* 97, 7396.
Shapiro, M., and Bony, H. (1985). *J. Chem. Phys.* 83, 1588.
Shapiro, M., and Brumer, P. (1987). *Faraday Disc. Chem. Soc.* 82, 177.
Shapiro, M., and Brumer, P. (1989). *J. Chem. Phys.* 90, 6179.
Shapiro, M., and Brumer, P. (1991). *J. Chem. Phys.* 95, 8658.
Shapiro, M., and Brumer, P. (1992). *J. Chem. Phys.* 97, 6259.
Shapiro, M., and Brumer, P. (1993). *Chem. Phys. Lett.* 208, 193.
Shapiro, M., and Brumer, P. (1993). *J. Chem. Phys.* 98, 201.

Shapiro, M., and Brumer, P. (1997). *Trans. Farad. Soc.* 93, 1263.
Shapiro, M., Hepburn, J. W., and Brumer, P. (1988). *Chem. Phys. Lett.* 149, 451.
Sheeny, B., Walker, R. B., and DiMauro, L. F. (1995). *Phys. Rev. Lett.* 74, 4799.
Shi, S., Woody, A., and Rabitz, H. (1988). *J. Chem. Phys.* 88, 6870.
Shi, S., and Rabitz, H. (1989). *Chem. Phys.* 139, 185.
Shnitman, A., Sofer, I., Golub, I., Yogev, A., Shapiro, M., Chen, Z., and Brumer, P. (1996). *Phys. Rev. Lett.* 76, 2886.
Szöke, A., Kulander, K. C., and Bardsley, J. N. (1991). *J. Phys. B.* 24, 3165.
Tannor, D., and Rice, S. A. (1985). *J. Chem. Phys.* 83, 5013.
Tannor, D., Kosloff, R., and Rice, S. A. (1986). *J. Chem. Phys.* 85, 5805.
Tannor, D. J., and Rice, S. A. (1988). *Adv. Chem. Phys.* 70, 441.
Taylor, J. R. (1972). *Scattering theory.* Wiley (New York).
Walker, D. C., ed. (1979). *Origins of optical activity in nature.* Elsevier (Amsterdam).
Wang, F., Chen, C., and Elliott, D. S. (1996). *Phys. Rev. Lett.* 77, 2416.
Wang, X., Bersohn, R., Takahashi, K., Kawasaki, M., and Kim, H. L. (1996). *J. Chem. Phys.* 105, 2992.
Warren, W. S., Rabitz, H., and Dahleh, M. (1993). *Science* 259, 1581.
Yan, Y., Gillilan, R. E., Whitnell, R. M., and Wilson, K. R. (1993). *J. Phys. Chem.* 97, 2320.
Woolley, R. G. (1975). *Adv. Phys.* 25, 27.
Yelin, D., Meshulach, D., and Silberberg, Y. (1997). *Opt. Lett.* 22, 1793.
Yin, Y.-Y., Chen, C., Elliott, D. S., and Smith, A. V. (1992). *Phys. Rev. Lett.* 69, 2353.
Yin, Y.-Y., Shehadeh, R., Elliott, D., and Grant, E. (1995). *Chem. Phys. Lett.* 241, 591.
Zhang, J. Z. H., and Miller, W. H. (1989). *J. Chem. Phys.* 91, 1528.
Zhu, L., Kleiman, V. D., Li, X., Lu, S., Trentelman, K., and Gordon, R.J. (1995). *Science* 270, 77.
Zhu, L., Suto, K., Fiss, J. A., Wada, R., Seideman, T., and Gordon, R. J. (1997). *Phys. Rev. Lett.* 79, 4108.
Zuo, T., and Bandrauk, A. D. (1996). *Phys. Rev. A* 54, 3254.